An investigation on local activity of convective precipitating cloud in Indonesia

村田，文絵

(Degree)
博士（理学）

(Date of Degree)
2003-03-31

(Date of Publication)
2008-05-30

(Resource Type)
doctoral thesis

(Report Number)
甲2777

(URL)
https://hdl.handle.net/20.500.14094/D1002777

博士論文

An Investigation on Local Activity of Convective Precipitating Cloud in Indonesia

(インドネシアにおける対流性降水雲の局地的活動度に関する研究)

平成１５年 １月

神戸大学自然科学研究科

村田 文絵

Acknowledgments

The author wishes to express her sincere appreciation to Professor Manabu D. Yamanaka for his continuous encouragement, helpful comments for scientific interests of Indonesian meteorology, giving many opportunities to experience observations and to participate international and domestic conferences, and supervision in the present work.

The author deeply thanks Professors Tadashi Mukai, Yoichiro Otofuji, and Kuniyosi Ebina for evaluating this thesis.

The author is grateful to Dr. Takahiro Iwayama for his adequate and important comments for the present work.

The author owe Dr. Hiroyuki Hashiguchi a debt of gratitude for his kind guidance for BLR technique and rawinsonde observations, his technical support regarding computer hardware and software, for his leadership to conduct intensive rawinsonde observations successfully and many useful discussions for the present work.

Special thanks are due to Dr. Shin-Ya Ogino for his many helpful suggestions on the way to advance the present work.

Special thanks are also due to Dr. Masatomo Fujiwara for his many valuable suggestions and comments regarding techniques to extract important information from observational results.

The author deeply thanks Dr. Noriko Okamoto for many useful discussions, her continuous efforts to keep comfortable environment of their laboratory, and continuous encouragement.

The author is greatly thanks Drs. Shuichi Mori, Jun-Ichi Hamada and Mr. Yudi Iman Tauhid for their leadership to conduct intensive rawinsonde observations successfully and for many useful discussions.

The author also wishes to express her hearty gratitude to Professor Shoichiro Fukao at RASC Kyoto University, Dr. Jun Matsumoto and Dr. Yoshiaki Shibagaki for careful reading the manuscript and their continuous encouragement regarding the present work.

The author express her hearty thanks to Mr. Sri Diharto, Director General of BMG for his kind permission to use the GAW observatory for our collaborative observations and Messrs. Eddy Kelana, Budi Suhardi, Ariyana Yasin, Antoyo S., Urip Haryoko, Nasrullar, Herizal, Imam Prawoto, Kaharudin, Charles, Darmadi for their cooperation through the intensive rawinsonde campaigns.

The author deeply thanks Miss Tien Sribimawati, Dr. Mahally Kudsy, Mrs. Sri Woro B. Harijono, Mr. Findy Renggono, and all colleagues of BPPT, and RASC Kyoto University for their collaborations throughout the intensive rawinsonde campaigns.

Thanks are due to Dr. Teruo Ohsawa and Mr. Noriyuki Nishi for providing the GMS IR data and helpful comments.

The author is grateful to all of persons who gave her helpful comments for her presentations in the congresses.

The author is indebted to all members of laboratory for atmosphere-hydrosphere sciences, Kobe University.

Abstract

Tropical convective activities play an important role on the global atmosphere through release of latent heat and wave generation. There are various time scales of convective activities. The temporal variations considered in this thesis are time scale from one day to 30–60 days (corresponding to intraseasonal oscillations). Since 1960s some of important phenomena peculiar to the equatorial regions, such as intraseasonal oscillations and equatorial waves, have been found and investigations for the mechanisms and their impacts on the global atmosphere have been activated. On the other hand, there are a few studies for the diurnal variation of convections. Indonesian maritime continent is one of the most active clouds regions in the world. The diurnal variation of convections is remarkable in this region because of the complicated land-sea distribution. In addition, the intraseasonal oscillations and some of equatorial waves are coupling to the convections and form the organized cloud systems in this region. In tropical regions number of meteorological stations and time resolutions of data are quite insufficient. In this thesis conditions of convective activities at Kototabang(0.20°S, 100.32°E, 865m MSL), which is located in the mountainous region of Sumatera Island, were analyzed by utilizing a boundary layer radar (hereafter referred as BLR) and other ground-based measurements.

A BLR has been operated at Kototabang since August 1998, and continuously provides three dimensional wind components up to 6.5 km with time resolution of 1 minute and height resolution of 100 m. The BLR can be regarded as a kind of rain gauge because it is sensitive to rain drops in rainy conditions. A determination method to obtain rainfall durations are shown. Comparison between NCEP/NCAR objective reanalysis data and BLR horizontal wind data are also indicated. At Kototabang total six intensive rawinsonde observation campaigns had been conducted by April 2002 (which were launched every four or eight times par day). Two observations periods, which is September–October 1998 and May–June 2001, were analyzed in this thesis (see Chapter 3). The surface meteorological instruments during August 1999–April 2002 were utilized by the statistical analysis (see Chapter 4). The database of GMS equivalent black body temperature and NCEP/NCAR objective reanalysis data also have been utilized.

Two case studies had been conducted. In the case study of September–October 1998 the correlations between westerlies of 1–3 km height range and precipitations at Kototabang have been found. The both westerlies and precipitations varied around 10-day periodicities. The precipitations were occurred by the local cloud systems which developed in the afternoon along the mountain range. The cloud systems more developed when the westerlies became weak. The development of local cloud systems was explained by the convergences of local winds, such as sea breezes or valley breezes under the geographical conditions. It was suggested that the strong background westerlies prevented the local circulations from developing, and as the results the precipitating local cloud systems did not easy to develop under strong westerlies. The cause of the 10-day periodicities observed during September–October 1998 were discussed. It is well known that the intraseasonal oscillations sometimes follow strong westerlies in the lower troposphere. It was considered that the westerlies strengthened during the passage of the intraseasonal oscillation and the n=1 equatorial waves embedded into the intraseasonal oscillation caused the 10-day periodicities. The correlations between westerlies and precipitations were observed during May–June 2001 too. In addition the variations of vertical distributions of temperature and humidity before and after strong westerly periods

had been observed. A half day to one day time lags were found for the correlations between westerlies and precipitations. These include another new results for the relationship between strong westerlies, eastward propagating mesoscale cloud systems, low tropospheric atmosphere drying, and the existence of large-scale convectively inactive regions after passing mesoscale cloud systems. However, their interpretations are still insufficient.

The statistical analysis have been made by utilizing 33-month data. The precipitations tended to occur when the westerlies were weak. The days of strong westerlies were clearly divided by rainy days with low solar radiations and no rainy days with high solar radiations. The rainy days with more than 30 mm daily rainfall amounts were selected for more detailed analysis. On one hand the rainfalls of weak westerly days occurred by the local cloud systems developing in the afternoon along the mountainous region. On the other hand the rainfalls of strong westerly days occurred under the large cloud systems by intraseasonal oscillations. The rainfalls during weak westerly periods were occupied large parts. It means that the rainfalls by the local cloud systems are dominant at Kototabang. It was considered that the reason why there are little rainfalls occurred by intraseasonal oscillations. There are a possibility that the transformations of the large cloud systems following intraseasonal oscillations, which were pointed out by Nitta *et al.* (1992), were occurred by the lifting effects of Sumatera mountain range acting the offshore convections.

Contents

List of Figures

List of Tables

Chapter 1

Introduction

1.1 Review for studies of convective activities around Indonesia

Indonesia is a region of the most active convection over the world. The convective clouds produce a large amount of latent heat in the processes of convert water vapor to liquid and solid. The latent heat produced in the Indonesian region drives the global-scale circulations, so called Hadley circulation and Walker circulation. The convection has variations of various time-scales. This study concerns the time scales from one day to intraseasonal (around 30–60 days).

Since the 1960s some of the important phenomena, e.g., the intraseasonal oscillations (ISOs) and the equatorial waves have been found (Madden and Julian, 1971), and so many investigators have analyzed and discussed about the mechanisms of the phenomena and the impacts to the global scale atmosphere. ISOs were found as eastward propagating west-east circulations having 30–60 day periodicities and their horizontal scales of several thousands kilometers, so sometimes referred as Madden-Julian oscillations (MJOs). ISOs are coupled with the active convections around Indonesian region. The equatorial waves are the disturbances appearing in the equatorial regions where the effect of Coriolis force is small or vanishes. The waves were led theoretically by Matsuno (1966) and were found observationally by Yanai and Maruyama (1966) and Wallace and Kousky (1968). The periodicities of these disturbances are from 1–2 days to 20 days. Some of these waves were coupled with the convection, and some studies utilizing satellite data have been done (e.g., Takayabu 1994, Wheller et al. 1999, 2000). Nakazawa (1988) showed that these disturbances (with different scales) interact with each other, and are organized to be a hierarchical structure.

In this study a relation between convections and lower tropospheric zonal wind variation will be argued. For zonal wind variation, it has been well known since Madden and Julian (1971) that zonal wind of the lower troposphere (around 850 hPa pressure level or 1.5 km above sea level) and of the upper troposphere (around 200 hPa pressure level or 12 km above sea level) often have 30–60 days periodicities corresponding to ISOs. Some of the equatorial waves also produce shorter variation of zonal wind on the equator. In observations and objective analysis strong westerly wind more than 10 m/s, of which time scales are from several days to several ten days, have been analyzed (Keen, 1982, 1988; Nitta and Motoki, 1987). The

strong westerlies are often correlated to cloud activities, and active convection is located on the eastern ends of the strong westerlies. Keen (1982) considered the relationship between strong westerlies and twin cyclones which are two symmetrical cyclones to the equator. Nitta and Motoki (1987) noticed ISOs as a trigger of El Niño events. It was regarded that the strong westerlies were one of important features prior to El Niño (Lau et al, 1989).

It has been observed by rain gauges (Gray and Jacobson, 1977; Oki and Musiake, 1994) and satellites (Hendon and Woodberry, 1993; Nitta and Sekine, 1994) that the diurnal variations of rainfalls and convective activities are remarkable in the tropical regions. The amplitudes of diurnal variations are large over the land area such as Africa, south America and Indonesia, and are small in the oceanic region. The phases of diurnal variations are completely different region by region and may be affected by the land-sea distributions and topography (e.g. Ohsawa et al. 2001). Houze et al. (1981) discussed offshore convection in the morning as a convergence of land breeze and monsoon flow by utilizing the radar observations, satellite images and pilot-balloon data in North Borneo. However, studies describing mechanisms of cloud development and rainfall are scarce because information on the distributions of wind, temperature, humidity and their time evolutions associated with the cloud systems was generally quite insufficient in the tropical regions.

The Indonesian maritime continent is located in the 'warm pool' region where the sea surface temperature is the highest all over the world. Over this region the ISOs and the equatorial waves are coupling with the convections. The importance of the 'warm pool' region had been suggested, and an intensive observational project TOGA-COARE(Tropical Ocean and Global Atmosphere - Coupled Ocean-Atmosphere Response Experiment) was carried out (Webster and Lukas, 1992). Many aspects of studies for convective activities have been done, for example, the structure and evolution of the ISOs (Yanai et al., 2000), quasi-two-day disturbances which were regarded as one of the equatorial waves by Takayabu (1996), the relation with the low-level westerlies (Lin and Johnson, 1996) and diurnal variation (Chen and Houze, 1997; Kubota and Nitta, 2001).

However, most of the observational area of TOGA-COARE, bordered by 10°N,10°S, 140°E and the date line, was occupied by the ocean, although the land-sea distribution is complicated over the Indonesian maritime continent. Such a difference of geographical conditions may produce the amplitude differences of diurnal variations of convection. The striking diurnal variations of convective activities over Indonesia is one of the important features (Nitta and Sekine, 1994).

In Indonesia reliable observational data had been quite insufficient. Hamada et al. (2002) collected and constructed database of the daily rainfall data over Indonesia and classified the seasonal variation of rainfalls at each of the regions into some categories. They also discussed the difference between El Niño and La Niña years. However, the rainfall data which can resolve diurnal variations are now collected, after installations of automatic rain gauges at several points in the mountain range of Sumatera.

For other meteorological variables the operational rawinsonde data of 11 stations in Indonesia have been collected, and confirmation of the reliabilities and construction of a database have been made by Okamoto et al. (2002) in parallel with this investigation. At some regions intensive rawinsonde observations have been carried out (Tsuda et al., 1994; Shimizu and Tsuda, 1997; Fujiwara and Kita, 2000). However, observations with high time resolution for a longer term are incompatible because of the necessity of man power.

In November 1992 a boundary layer radar (hereafter referred as 'BLR') was constructed at Serpong (6.4°S, 106.7°E, 50 m MSL) near Jakarta, West Java, Indonesia. BLR is a 1.3 GHz wind profiler, with which we can observe horizontal wind velocity until about 6.5 km above the ground and several studies related to cloud convection systems have been carried out (Hashiguchi et al., 1995, 1996; Widiyatmi et al., 1999). In August 1998 a similar type of BLR had been installed at Kototabang near Bukittinggi, West Sumatera (0.20°S, 100.32°E, 865 m MSL). A difference between Serpong and Kototabang is their geographical conditions. Serpong is located in a plain, but Kototabang is located in a mountainous region. On both BLR sites automatic surface meteorological instruments also have been operated. Moreover, BLRs detect the precipitation particle motion on rainy conditions. At Kototabang, the several intensive rawinsonde observations had been conducted and the vertical structure of thermodynamics had been obtained. As a result, the high time resolution data from which we could analyze the diurnal variations were obtained at Kototabang for longer periods. The author has been a member of these intensive observations.

1.2 Contents of the thesis

This thesis concerns variations of rainfall at Kototabang (100.32°E, 0.2°S, 865m MSL), west Sumatera, Indonesia and especially, relationship between them and lower-tropospheric wind varying with diurnal variations and with ISOs.

In Chapter 2, the observations and datasets employed in this investigation, which are BLR, GPS rawinsondes, surface meteorological instruments, GMS and NCEP reanalysis, are described. A determination method of rainfall from BLR data is proposed and a comparison between BLR and NCEP reanalysis data is carried out.

In Chapter 3, results obtained during two intensive observation periods are presented. A correlation between precipitation and lower-tropospheric westerly, which is the main issue in this thesis, is firstly described based on data analysis for an observation period, and a plausible explanation is presented in Section 3.1. The causes of zonal wind variations are examined in Section 3.2. Data obtained during another intensive observation period are analyzed, and the similarities and differences with the results of first case study are discussed in Section 3.3.

In Chapter 4, the correlation between low-level westerly and precipitation at Kototabang is examined statistically by using nearly three-year data in Section 4.1. Dominant cloud systems which cause much precipitation at Kototabang and are discussed in Section 4.2. Effects of Sumatera mountain range are considered in Section 4.3.

The summary and conclusions of this thesis are presented in Chapter 5.

Chapter 2

Description on observations and data

In this chapter, the observations and database utilized in this study are described in detail. An introduction of observation site are shown in Section 2.1. BLR (see Section 2.2), intensive rawinsondes observations(see Section 2.3), surface measurements (see Section 2.4) have been operated at Kototabang. Some database which are utilized to know horizontal information are described in Section 2.5.

2.1 Observation site

Kototabang (100.32°E, 0.20°S, 865 m above mean sea level) is located on a small hill in mountanious region (Barisan Mountains) along west coast of Sumatera Island. The distance from Indian Ocean is around 50 km. There are a traditional city of 'Minan Kabau', Bukittinggi in around 30 km south of Kototabang. Two large mountains more than 3000 m, 'Mt. Singgalang' and 'Mt. Marapi', exist in the south and south-east directions and 30–40 km away from Kototabang. Small mountains extend from north to north-east of Kototabang, and also there are a lake 'Maninjau' surrouded by small mountains in the west direction. This observation site was found and opened in order to construction of large-size radar, and now 'Equatorial Atmosphere Radar' have been operated since July 2001. Global Atmosphere Watch (GAW) station had constructed on this site by World Meteorological Organization in 1996 and surface meteorological observations and trace gas observations have been operated. Climatological annual rainfalls of West Sumatera are 2000–4000 mm. There are two rainy seasons in the equinoxes, which are March–May and September–November (Inoue and Nakamura, 1990; Hamada, 2002). Rainfalls of September–November tend to excess that of March–May. The seasonal variation of rainfalls correspond to north-south transition of ITCZ along 100°E (Murakami and Matsumoto, 1994).

Routine rawinsonde observations have been operated at Tabing (0.88°S, 100.35°E, 2m MSL) near Padang city, where is located around 100 km south of Kototabang and facing Indian Ocean. The operational rawinsonde data have been collected and analyzed by Okamoto et al.(2003). Based on their results, zonal wind in lower troposphere (less than 8 km altitude) at Padang is westerly throughout a year. In upper troposphere easterly wind is dominant and has semiannual periodicity, which becomes maximum in January–February and in July–August. It is thought to be due to the transport of easterly wind momentum by Hadlay circulation

under conservation of angular momentum. The easterly wind momentum originally comes from intensified Walker circulation in summer hemisphere (Okamoto et al., 2003). For meridional wind annual variation in upper troposphere (southerly in boreal winter and northerly in boreal summer) is dominant, and which is correpond to Hadley circutation.

2.2 Boundary layer radar (BLR)

A 1.3GHz (UHF or *L*-band) boundary layer radar (BLR) with a peak transmitter power of 1kW was installed beside the GAW station house at Kototabang (100.32°E, 0.20°S, 865 mMSL, see Fig. 2.1) in August 1998. The clear-air echoes are induced by refractive index fluctuations due to atmospheric turbulences, and spatial differences of temperature and humidity (see e.g., Gage et.al., 1990), and they provide information on atmospheric motions in clear air by the Doppler principle. The BLR has one parabolic antenna of 2m diameter and which is steered toward three directions (vertical, northward and eastward) mechanically to obtain three dimensional wind components. The observation range of BLR is from around 0.6 km to 2 or 3 km on clear air condition and 6.5 km (which corresponds to the maximum sampling height) on rainy condition with 1 minute time resolution and 100 m height resolution. The radio waves with this frequency band are reflected with much greater echo intensity for precipitation particles than that for the atmosphere during rainfall. Because the vertical Doppler velocity due to falling precipitation particles is as large as several m/s, it can be distinguished from the atmospheric vertical motion (normally less than 1 m/s). For these reasons, the rainfall duration has been determined by the data of BLR vertical Doppler velocity and BLR echo power, as will be described in Section 2.2.1.

BLR had been operated continuously during the analysis period of first case study (September–October 1998; see Section 3.1, 3.2), except for short periods of the electric power shortage. For statistical analysis (see Chapter 4) horizontal winds of NCEP reanalysis are utilized because of many missing data. Comparison between NCEP and BLR is represented in Section 2.2.2.

Specification of the BLR system and typical observation parameters are described in Table 2.1. Further details on BLR have been described in Hashiguchi et al. (1995, 1996) and Renggono et al. (2001).

2.2.1 Determination of rainfall durations

The precipitation echoes detected with BLR are much stronger than clear air echoes (Gage 1990; Hashiguchi et al. 1995; Renggono et al. 2001). The BLR Doppler velocity due to falling precipitation particles becomes as large as several m/s, which is much larger than that of usual atmospheric vertical motion. Consequently, rainfall can be detected by using both the echo power intensity, and the vertical Doppler velocity observed with BLR. Algorithms to distinguish precipitation echoes from atmospheric echoes by the magnitude of echo power intensity have been developed at Kyoto University.[1]

[1]Tan, T. K., 1995: A study on the algorithm for distinction of non-atmospheric echoes observed with an *L*-band clear-air doppler radar. Bachelor's thesis, Department of Electronic Engineering, Kyoto university, 38pp.

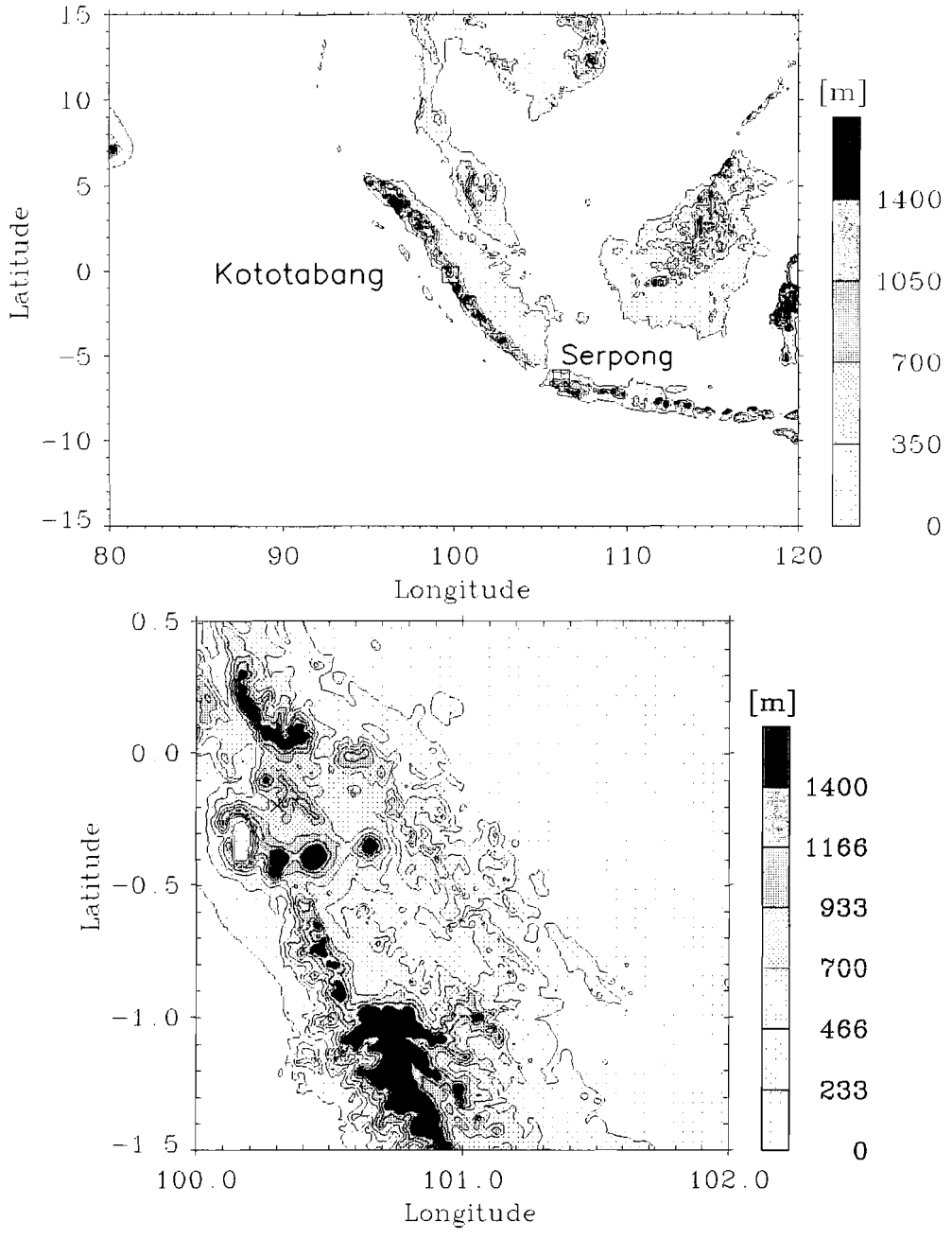

Figure 2.1: Upper panel is a geographical map of BLR sites. Lower panel is a geographical map of around Kototabang (100.3°E, 0.2°S). The data were downloaded from the internet site of U.S.Geological Survey (http://www.edcdaac.usgs.gov /gtopo30/gtopo30.html).

Table 2.1: Specification of the BLR system and typical observation parameters of the BLR.

Radar system	Monostatic pulse radar
Operating frequency	1357.5 MHz
Antenna	mechanically rotated parabolic antenna
Aperture	3.1 m^2 (2 m in diameter)
Beamwidth	7.6°(half power)
Beamdirections	(Azimuth, Zenith) = (0°, 0°), (0°, 15°), (90°, 15°)
Transmitter	
Peak power	1 kW (maximum)
Average power	20 W (duty ratio 2.0 %)
Bandwidth	4 MHz
Pulselength	1 μs (typical value)
IPP	50 μs (typical value)
Range resolution	100 m
Maximum observable horizontal wind velocity	67.1 ms^{-1}
Resolution of horizontal wind velocity	1.0 ms^{-1}

The time interval and height range used for the determination of rainfall durations were selected by the following reasons: Ice crystals may exist above the melting layer at around 4 km. The observed radar echo intensity below 2 km is underestimated due to saturation in the dynamic range of the radar receiver. We selected 2–3 km as the height range for rainfall determination. The rainfall intensity by a tipping-bucket-type rain gauge, which was utilized to compare with BLR echoes, is determined on the assumption that the rainfalls occur uniformly during the counts of tipping of the bucket. The time resolutions (1 min) of both BLR and the rain gauge are too short for normal rainfall to full the volume (0.5 mm) of the rain gauge bucket, and the lifetime of a convective cloud is sufficiently within 1 hour. Consequently, we took 10 min as the time interval for rainfall determination.

Figure 2.2(a) shows a distribution of vertical Doppler velocity versus echo power intensity during 27 September–7 October 1998, which corresponds to the first simultaneous observation period with rain gauge. Positive and negative values of the vertical Doppler velocity are downward and upward, respectively. Each data sample was averaged for 2–3 km in height, and for 10 min in time. Remarkable rainfalls observed by the rain gauge simultaneously are also indicated. Weak echo power intensities concentrated near the zero Doppler velocity correspond to the clear air echoes. On the other hand, precipitation echoes have large Doppler velocities and show strong echo power intensities.

Based on this distribution, we determined threshold values to discriminate atmospheric and raindrop echoes as '0 dB' for the echo power, and '1 m/s' for the Doppler velocity. Figures2.2(b) and (c) show a comparison between rainfall intensity observed by the rain gauge and the rainfall duration determined by the BLR echoes. Both the results are in good coincidence with each other. It should be mentioned that the BLR echo method is not always useful when the rainfall intensity is very weak, when the precipitating clouds have very low cloud-base (below 2 km),

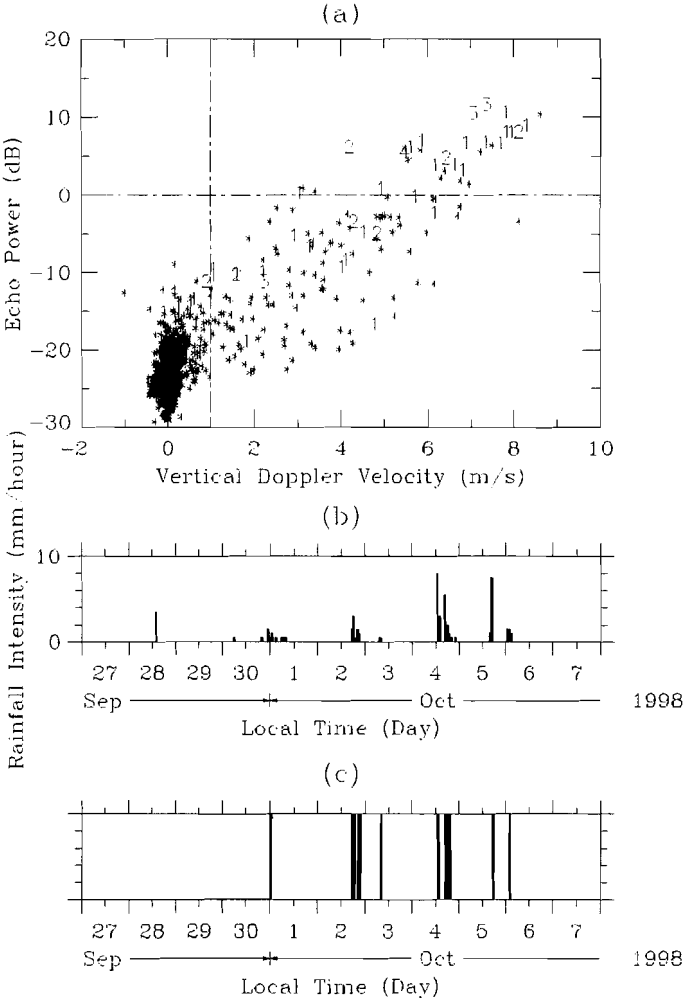

Figure 2.2: (a) A distribution of BLR vertical Doppler velocity versus BLR echo power intensity during the intensive observation period. Positive and negative values of the vertical Doppler velocity are downward and upward, respectively. Each point was the data averaged for 2–3 km in height and for 10 min in time. '1', '2', '3' and '4' denote rainfall intensities (observed by a rain gauge simultaneously) of 0.5–1.0, 1.0–3.0, 3.0–6.0 and $\geq$6.0 mm/10 min. (b) Rainfall amount (per 1 hour) by the rain gauge. (c) Rainfall durations decided by BLR. these are shown every 1 hour, which contain more than one decided rainfall durations by every 10 min.

or when the precipitation occurs on a short time ($\ll$ 10 min).

Using the method mentioned above, the determination of precipitation durations is extended two months, September–October 1998 (see Fig.3.1(b) of Section 3.1.1).

2.2.2 Comparison with NCEP reanalysis data

The daily averaged BLR zonal wind are compared with the 700 hPa level NCEP reanalysis data of the nearest grid point at Kototabang (0°, 100°E) in Fig. 2.3. The detailed explanations of NCEP reanalysis data are described in Section2.5.

The upper figure of Fig. 2.3 shows a comparison between time series during August 1998–July 1999. Thick line and thin line represent BLR zonal wind of 1.6–2.5 km heights (2.5–3.4 km above mean sea level) and 700 hPa (around 3 km above mean sea level) level NCEP reanalysis data, respectively. The both lines are almost good coincident with each other, except for the amplitudes of BLR are a little larger than NCEP data. The lower figure of Fig. 2.3(b) is a scatter plot of BLR data versus NCEP data. The line ,which is best fitting to the distribution, is y = 0.85x - 0.49, which means that NCEP data has a bias of -0.5 m/s and the absolute value tend to be lower by 15%.

The values of NCEP reanalysis are the representative over 2.5°grid (around 250 km) square. The values of BLR are the representative over the order of 0.01 km square just above Kototabang. However, the both values and variations were good correlations with each other. This gives two insights. Firstly, it implies that the daily averaged winds above Kototabang are controlled by the large scale background disturbances. Secondly, it is available to utilize NCEP data to examine the variations of daily averaged wind observed at Kototabang. In Chapter4, NCEP values are utilized because of many missing data of BLR.

2.3 Description on intensive rawinsonde observations

At Kototabang total six intensive rawinsonde observations had been operated by Kobe University during August 1998–April 2002. First two intensive observation periods (IOPs) were conducted in cooperation with RASC Kyoto University, Kobe University, University of Tokyo, Agency for the Assessment and Application of Technology (BPPT) and Indonesian Meteorological and Geophysical Agency (BMG) during 27 September– 7 October. 1998 (rainy season) and 8–14 August 1999 (dry season), although the second IOP were cancelled because of the receiver trouble. The main purpose of these IOP was the mutual comparison to the BLR which had been installed August 1998. In the first IOP several ozonesondes launched by University of Tokyo combined with airborne observation BIBLE-A campaign which observed three dimensional distributions of ozone and ozone precursors. The first IOP also corresponds to the end of GAME (GEWEX Asian Monsoon Experiment) IOP (April–September 1998) which had been conducted in monsoon Asia region covering Indo-china peninsula to Siberia.

The third to sixth observations had been operated by Frontier Observation Research System for Global Change (FORSGC), Kobe University, BPPT and BMG during 17 May–12 June (transition season from rainy to dry season), 1–28 August (dry season), 1–28 November (one of two rainy season) 2001 and 2–29 April 2002 (another rainy season). In the fifth and sixth IOP simultaneous rawinsonde observations had been carried out at Jambi (1.63°S, 103.64°E, 26m

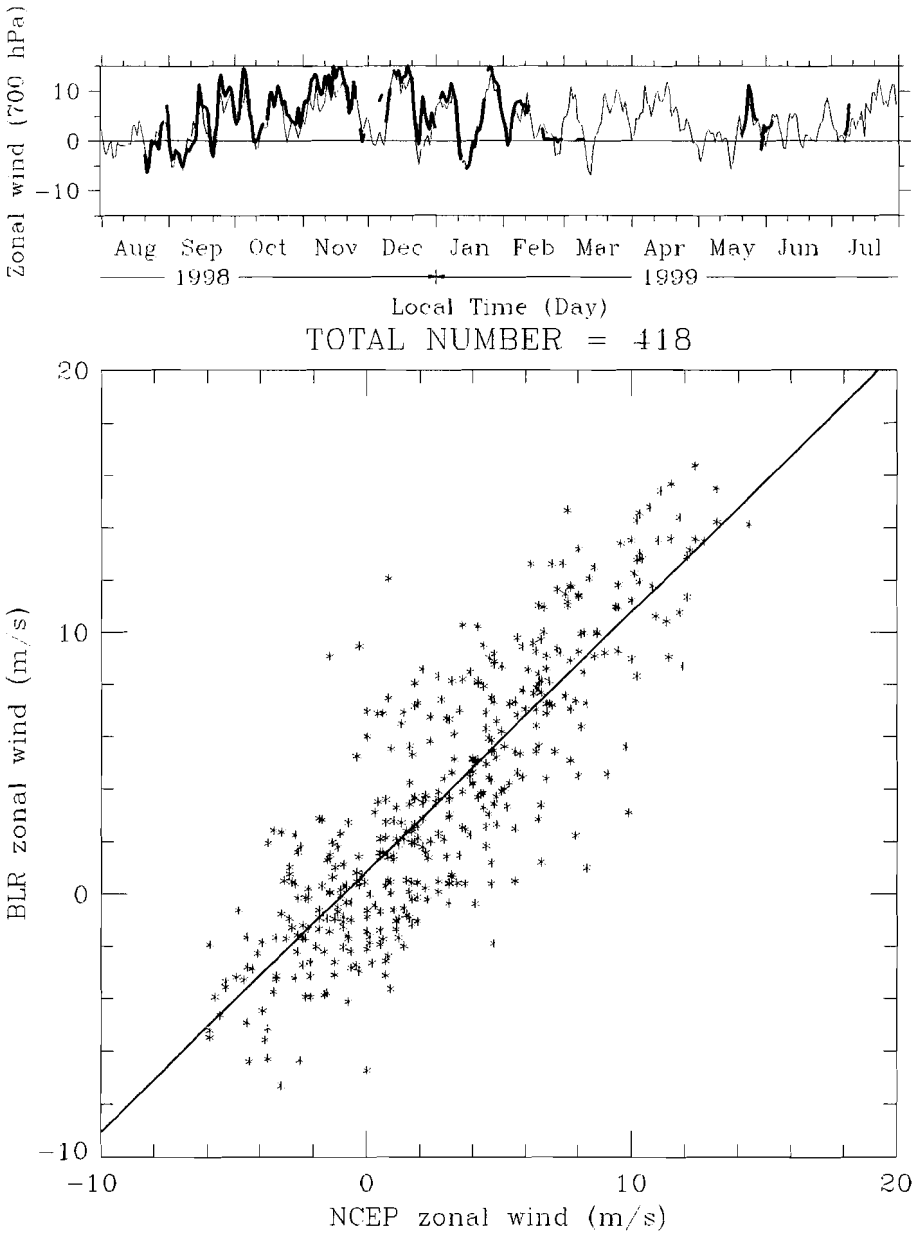

Figure 2.3: The comparison between BLR zonal wind and NCEP reanalysis data. Upper figure is time series during August 1998–July 1999. Thin and thick lines represent BLR zonal wind of 1.6–2.5 km heights (2.5–3.4 km above mean sea level) and 700 hPa (around 3 km above mean sea level) level NCEP reanalysis data, respectively. Lower figure is scatter plot of BLR zonal wind and NCEP reanalysis data.

MSL, east of Sumatera mountainous region) during 1–28 November 2001 and 4–25 April 2002 and Tabing (0.88°S, 100.35°E, 2m MSL) in the suburbs of Padang city (west of Sumatera and facing the Indian Ocean) during 12–18 November 2001 and 12–18 April 2002. The aim of IOPs were to understand seasonal variation in the atmosphere of this area and to reveal the deference between stations in Sumatera Island. These observational data were also utilized to evaluate EAR which had started operation since June 2001. The GPS water vapor observations and stable isotope observations have been started and continued over Sumatera and other Indonesia regions on a parallel with these IOPs.

GPS rawinsondes provide vertical profiles of pressure, temperature, humidity and horizontal wind up to around 30 km. The horizontal winds are detected by the change of sonde position measured by GPS (Global Positioning System). In first IOP we employed an AIR GPSonde sounding system with meteorological balloons (TA-1000 type for daytime, and TX-1000 for nighttime) provided by TOTEX Co. Ltd.. TX-1000 is an improved type balloon for the balloon burst around the tropopause(around 16–18 km) where temperature sometimes becomes lower than -80°C. They were launched four times a day at 0030, 0630, 1230 and 1830 LST (corresponding to observations for 1800, 0000, 0600 and 1200 GMT, respectively), except for 27 and 28 September on which the launch was done once per day (1630 and 1230 LST, respectively).

In third to sixth IOP the receivers and transmitters by Vaisala company were employed at Kototabang and Jambi. They utilized MW15 type receiver at Kototabang and MW21 type at Jambi. a Vaisala RS80-15GH radiosondes(equipped with a Global Positioning System(GPS) antenna for the horizontal wind measurement and a Humicap-H type relative humidity sensor which data is available up to around 12–13 km) are utilized with meteorological balloons (TA-1000 type for daytime, and TX-1000 for nighttime) provided by TOTEX Co. Ltd.. In addition to the use of TX-1000 balloon, we put the balloon into kerosene for around three minutes before launching, in order to lessen the number of balloon burst in low altitude. They were launched eight times a day at 0030, 0330, 0630, 0930, 1230, 1530, 1830 and 2130 LST (corresponding to observations for 1800, 2100, 0000, 0300, 0600, 0900, 1200 and 1500 GMT, respectively) during second and third weeks (24 May–5 June, 8–21 August, 8–21 November 2001 and 9–22 April 2002), and four times a day during other days.

At Tabing which is one of the operational rawinsonde observation sites in Indonesia and usually observe one times per day, four times a day observations had been conducted. The sounding system and transmitters made by Meisei company have been operated. The transmitter type was RS third 89 with 600g balloon, which was lighter than other stations, however, normally reached up to 30 km.

In this thesis two IOPs which is observed at Kototabang are analyzed (see Chapter 3).

2.4 Surface measurements

(a) Rain gauge measurement

We used a standard tipping-bucket-type rain gauge (produced by Ogasawara Co. Ltd.) during 27 September–7 October 1998. The minimum sensitivity for rainfall amount was 0.5 mm, and the temporal resolution of the recorded data was 1 min. The rain gauge was put on the roof of the GAW station building, which was just on the neighborhood of the BLR antenna.

(b) Standard operational measurements

The data of surface temperature, pressure, and relative humidity used in this study were provided from standard operational observations (barograph and thermohygrograph) at the GAW station. Two-month data during 00 LST on 1 September–23 LST on 31 October 1998 were used. They were sampled every hour on the hour.

(c) Automatic weather station

An automatic weather station, which was provided by Vaisala company(product type: MAWS 201), have been operated since August 1999 on the roof of the GAW station building, which was just on the neighborhood of the BLR antenna. It observes pressure (silicon capacitive pressure sensor), temperature (resistive platinum sensor), relative humidity(polymer sensor), global solar radiation (photodiode type pyranometer), wind speed and wind direction (combined wind vane and rotating cup anemometer) and rainfall amount (tipping-bucket-type rain gauge). The temperature and humidity sensors were protected by solar shield. The minimum sensitivity of the rain gauge was 0.2 mm. The solar panel was attached to secure from electric power shortage. The all measurements are recorded by every 1 minute.

2.5 Other data

(a) Satellite cloud data

GMS (Geostationary Meteorological Satellite) is a geosynchronous satellite operated by Japan Meteorological Agency (JMA). It is located on 140°E above the equator and is 35786 km away from the earth. GMS-5 have been carried out since 1995. Its VISSR (Visible and infrared spin scan radiometer) observes one visible and near-infrared (0.55–0.9 μm) and three infrared (10.5–11.5, 11.5–12.5, 6.5–7.0 μm) wavelengh bands or channels of reflective and radiative energy from the earth. The wavelength band nearby 11 μm is almost transparence for the earth atmosphere, then the radiation from earth surfaces and clouds, which are regarded as black body, can be observed. A brightness temperature of 10.5–11.5 μm wavelength band is often called 'equivallent black body temperature' (T_{BB}). The spatial resolution of infrared channel is 5 km just below the satellite and go down around 7–8 km at 100°E and around 10 km at 80°E for roundness of the earth. The time resolution is one hour. The data for September–October 1998 were obtained through the Disaster Prevention Research Institute, Kyoto University. For other months they were obtained through RASC Kyoto University, which is originally downloaded from following internet site, courtesy of Kochi University and Institute of Industrial Science, University of Tokyo.

`http://weather.is.kochi-u.ac.jp/`

(b) Objective analysis data

An objective analysis is a method of inserting meteorological values at a certain time into regularly arranged points (grid points) on the map objectively with uniform accuracy. Various observations, such as surface observations, upper air observations, data observed by vessels and by satellites, are setted in objective analyses. As the observations distribute ununiformly and have various range of accuracy, they are compared with 6 hour forecast values (often called 'first guess') of numerical forecasting model. The forecast values are inserted for an area where

observations are sparse. This method is in general called four dimensional assimilation. A numerical forecasting model is a program to forecast atmosphere conditions following to the governing laws of atmospheric motions. They compose parts of a forecasting system.

NCEP/NCAR (National Centers for Environmental Prediction / National Center for Atmospheric Research) of United States have been carried on a reanalysis project in 1990s. A developed numerical forecasting system was applied to the past weathers in order to obtain a uniform data sets that did not depend on the differences of foregoing operational systems. NCEP/NCAR reanalysis data assimilation system, which was utilized past 40 year reanalysis, have been operated since 1995 until present to monitor the climate change of the earth.

Chapter 3

Case studies

In this chapter, the results of two intensive observation periods are described. Firstly, the results during September–October 1998 are presented in Section3.1. A correlation between precipitation and lower tropospheric zonal wind, which is the main issue of this study is found in this period. The causes of lower tropospheric zonal wind variation are discussed in Section3.2. Another case study during May–June 2001 is presented in Section3.3.

3.1 Case study 1: September–October 1998

In this section results obtained during September–October 1998 are described. We mainly focus ourselves into a relationship between rainfall and wind variations, which is suggested first from results obtained during the two-week intensive observation period, and the period are extended to the two months as will be described in Section 3.1.1. The observational results at Kototabang are compared with the horizontal distributions of GMS cloudiness data and NCEP reanalysis wind data in Section 3.1.2. The discussions for the obtained results are described in Section 3.1.3

3.1.1 Observational results

Figure 3.1 shows the results of the intensive observation with BLR, GPS rawinsondes and the rain gauge. Figures 3.1(a) and (b) are time-height cross sections of zonal wind observed by rawinsondes and by BLR, respectively. In this period westerly wind is dominant below 6 or 7 km, and is especially strong below 3 km. From 29 September to the daytime of 2 October, and after the daytime of 5 October, westerly wind stronger than 10 m/s appears below 3 km. Figures 3.1(c) and (d) are variations of BLR echo power and rain intensity by the rain gauge. Strong BLR echoes shown in the former correspond to heavy rain, as mentioned in Section 2.2.1. Precipitations do not occur every day, and that stronger than 2 mm/hour are concentrated during the afternoon of 2–5 October, which is the weak westerly period suggested in Figs. 3.1(a) and (b). Therefore, the westerly wind variation is anti-correlated to precipitation.

Figure 3.1(e) shows time-height variation of equivalent potential temperature by rawinsondes. The equivalent potential temperature below 3 km generally shows convective instability

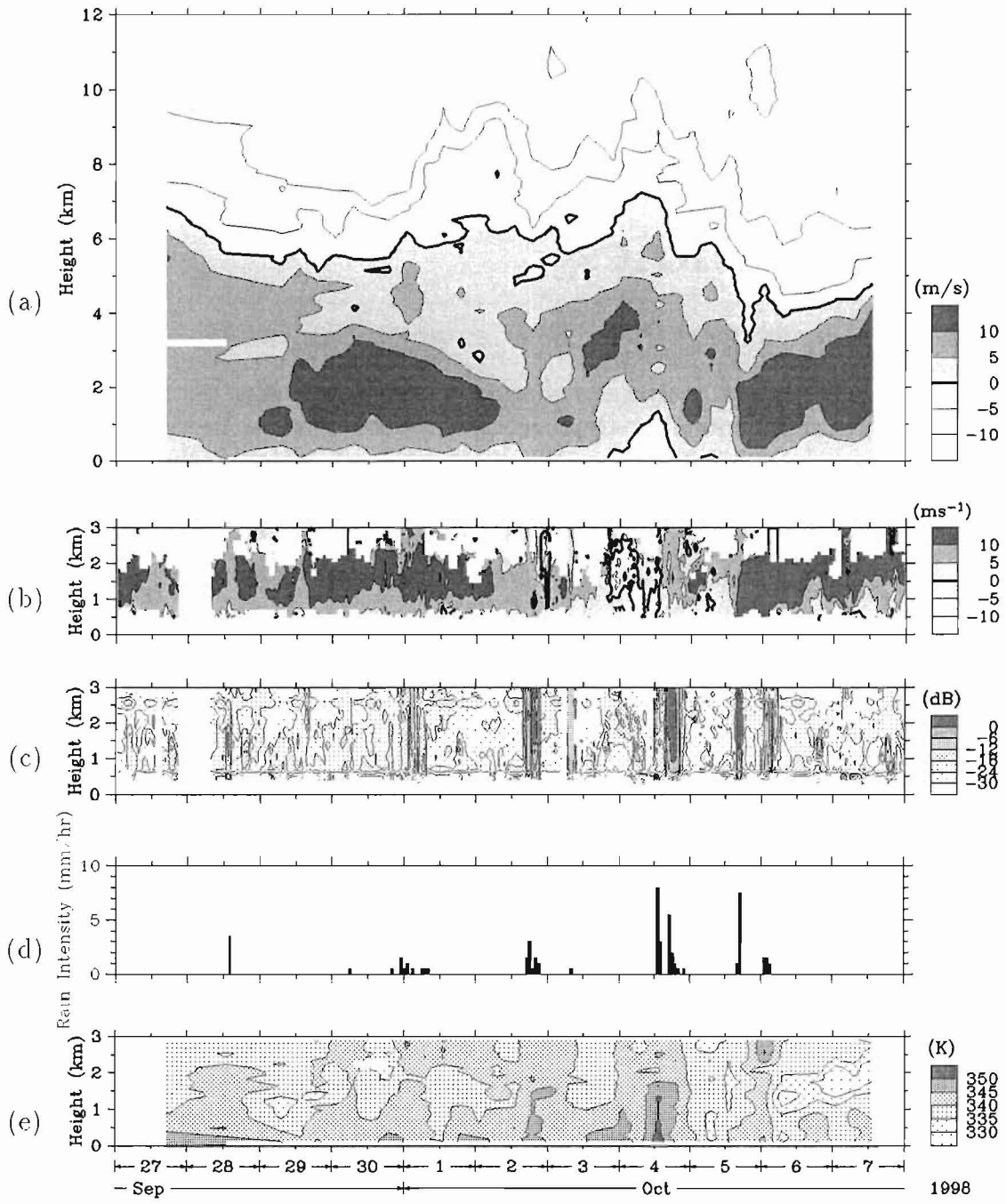

Figure 3.1: Results of the intensive observation period during 27 September–7 October 1998. Time-height cross-sections of zonal wind observed (a) by rawinsondes launched 4 times per day and (b) by BLR (60-min averaged). (c) 60-min averaged BLR echo power intensity. (d) Surface rainfall intensity observed by a rain gauge. (e) Time-height cross-section of equivalent potential temperature observed by rawinsondes.

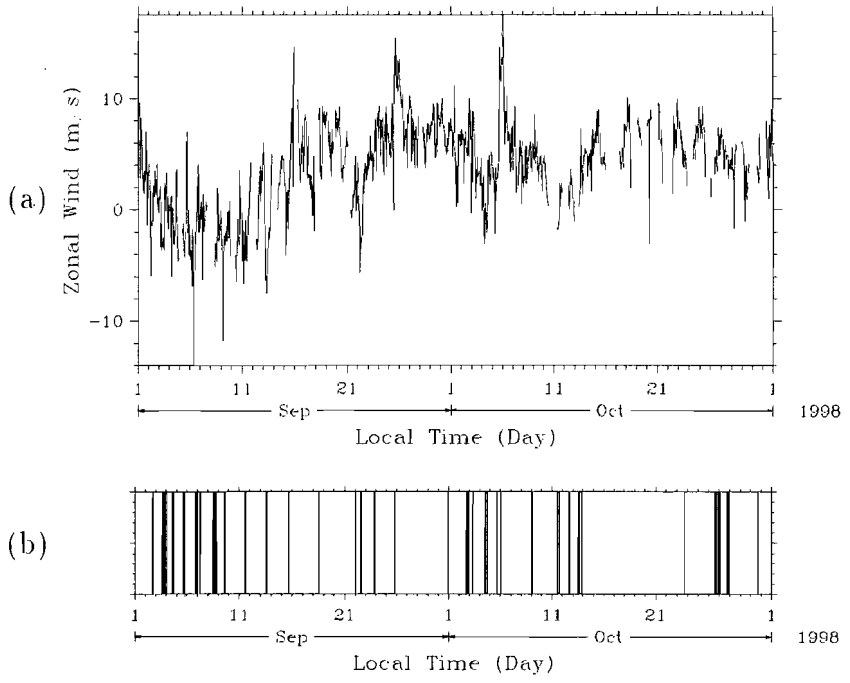

Figure 3.2: Results of two months during September–October 1998. (a) Time series of 60-min averaged zonal wind (averaged over 1–2 km height range). (b) Rainfall durations decided by BLR.

during the intensive observation period. This is the typical stratification in the tropical region (see e.g., Fig. 11.1 of Holton 1992). During the weak westerly period the equivalent potential temperature is decreased uniformly in vertical, it implies that the atmosphere has been mixed by convection. When the westerly wind is strong, the equivalent potential temperature is minimum at 1–2 km.

Figure 3.2 shows the zonal wind variation (averaged over 1–2 km height range), and the rainfall durations observed by BLR during September–October 1998. The rainfall durations during the two months are also correlated to the weak westerly periods, as suggested in the two-week intensive observation period. In particular, during 15 September–15 October, the zonal wind varies with a periodicity of about 10 days. The rainfall also has a similar periodicity.

Spectral analysis has been made to confirm the quasi-10-day periodicity. Figure 3.3 shows the energy-content form of power spectral densities calculated for zonal, and meridional, wind components averaged for 1–2 km height range during September–October 1998. A peak of 8–10 days is obvious for the zonal wind. The meridional wind also has a clear peak around 10–20 days, but the spectral amplitude is much smaller than that of the zonal wind. The diurnal component of meridional wind variation has a similar amplitude to the quasi-10-day component, but that of zonal wind variation is weak. A 3–4 day component is also found for both the zonal and meridional winds.

Figure 3.4 shows frequency power spectral densities for surface pressure, temperature and specific humidity. For all the variables the diurnal component is dominant, and a periodicity

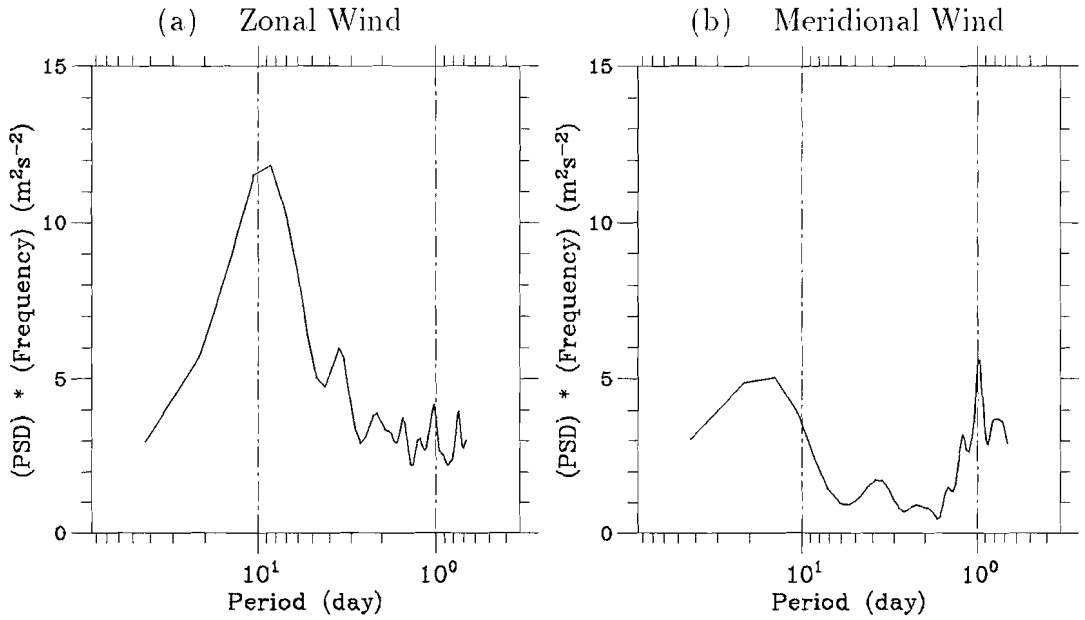

Figure 3.3: Spectral analyses of (a) BLR zonal wind and (b) BLR meridional wind averaged for 1–2 km height range. Vertical dashed-and-dotted lines indicate the diurnal oscillation (period of one day) and the 10-day periodicity.

of 2 days is found. Temperature and pressure have clear semi-diurnal periodicities, which may correspond to the atmospheric tide. A periodicity of 1.5 days appears in temperature and humidity, and a periodicity around 6 days is found for temperature. However, the 10-day component is generally very small in the surface meteorological quantities.

Therefore the spectral analyses for the lower-tropospheric wind, and the surface meteorological quantities, show existence of the diurnal component and the components with periods from a few days to about 20 days. After this we particularly notice the diurnal component, and the component of about 10 days, respectively.

On one hand, in order to examine the diurnal variation of rainfall, Figure 3.5 shows a histogram of precipitation for each hour at Kototabang during September–October 1998. The precipitation periods were determined by BLR (see Section 2.2.1). The occurrence of precipitation tends to be concentrated at 12–24 LST. This result is consistent with analysis for longer periods by Hamada et al. (2002) and Renggono et al. (2001). The maximum precipitation tends to occur during 16–18 LST.

On the other hand, the quasi-10-day periodicity was weak but appeared for all the parameters. To investigate the phase relationships between these parameters, a composite analysis is made for 7–13 day filtered BLR horizontal wind (averaged for 1–2 km height range), and surface meteorological variables (pressure, temperature and specific humidity) (see Fig. 3.6). The reference times are taken as 6 LST on 22 September, 16 LST on 3 October and 16 LST on 11 October, corresponding to minima of zonal wind. The phase differences to the zonal wind are 1/4 cycle for the meridional wind, 5/8 cycle for the pressure, 3/8 cycle for the temperature, and 1/2 cycle for the specific humidity.

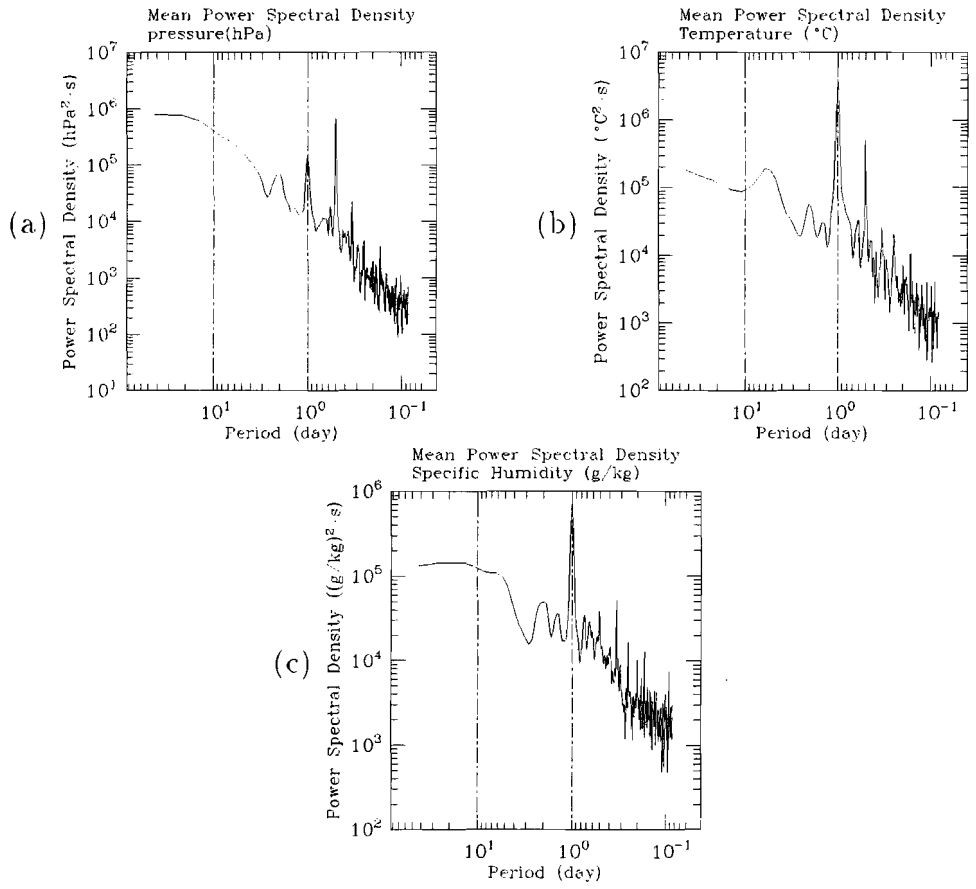

Figure 3.4: Spectral analyses of (a) surface pressure, (b) surface temperature and (c) surface specific humidity. Vertical dashed-and-dotted lines indicate the diurnal oscillation and the 10-day periodicity.

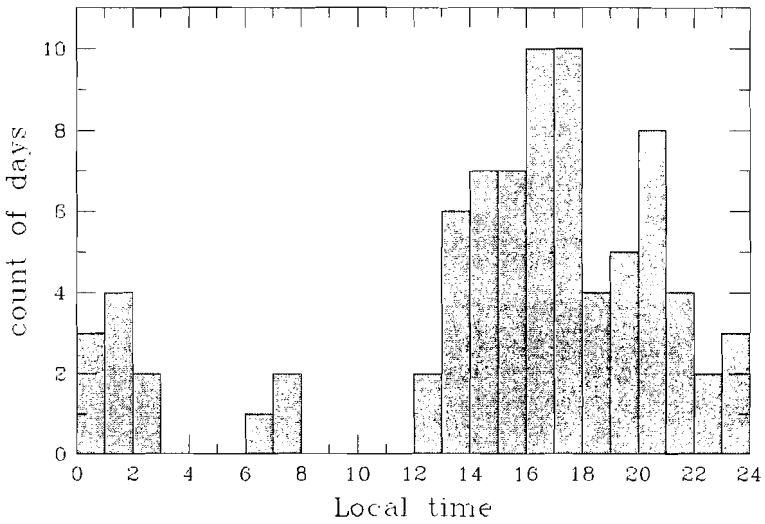

Figure 3.5: A Histogram of precipitation for each one hour at Kototabang during September–October 1998. The precipitations were decided by BLR.

3.1.2 Comparisons with horizontal distributions of zonal wind and clouds

In order to examine the horizontal scales of the quasi-10-day components found in the preceding section, the large-scale horizontal distributions of low-level zonal wind and developed clouds are analyzed in this section.

Figure 3.7(a) compares the BLR zonal wind averaged for the height range of 0.6–1.0 km (corresponds to the altitude range of 1.5–1.9 km from MSL) with NCEP 850 hPa data at the nearest grid point (0°, 100°E) to Kototabang. Both curves are quantitatively in good agreement. The quasi-10-day periodicity can be seen also in the NCEP data as less than 2 m/s zonal winds which correspond to the weak westerly periods at Kototabang during 15 September–15 October. Thus we utilize the NCEP data to investigate the zonal structure of the quasi-10-day periodicity. Figure 3.7(b) is the time-longitude cross section of zonal wind for 40–160°E along the equator. In this figure strong westerly wind appears in 70–100°E during 15 September–10 October and 20–31 October. Moreover, about 10-day periodicity appears in each period. However, the correlation with the quasi-10-day periodicity at Kototabang is unclear. Another remarkable point is that these strong wind regions do not continue eastward beyond 100°E. The zonal wind field is different between the both sides of 100°E.

Next the rainfall durations at Kototabang are compared with the time-longitude cross section of the 12-hourly GMS T_{BB} data (Fig. 3.8). The T_{BB} data are averaged in 2.6°S–2.6°N. In this period the two large-scale disturbances appear in 80–100°E: One appears during 11 September–6 October, and the other appears during 22–31 October. However, the rainfalls at Kototabang are hardly correlated with the cloud images. This suggests a peculiarity of the precipitation at Kototabang. The T_{BB} data also show a difference between both sides of 100°E.

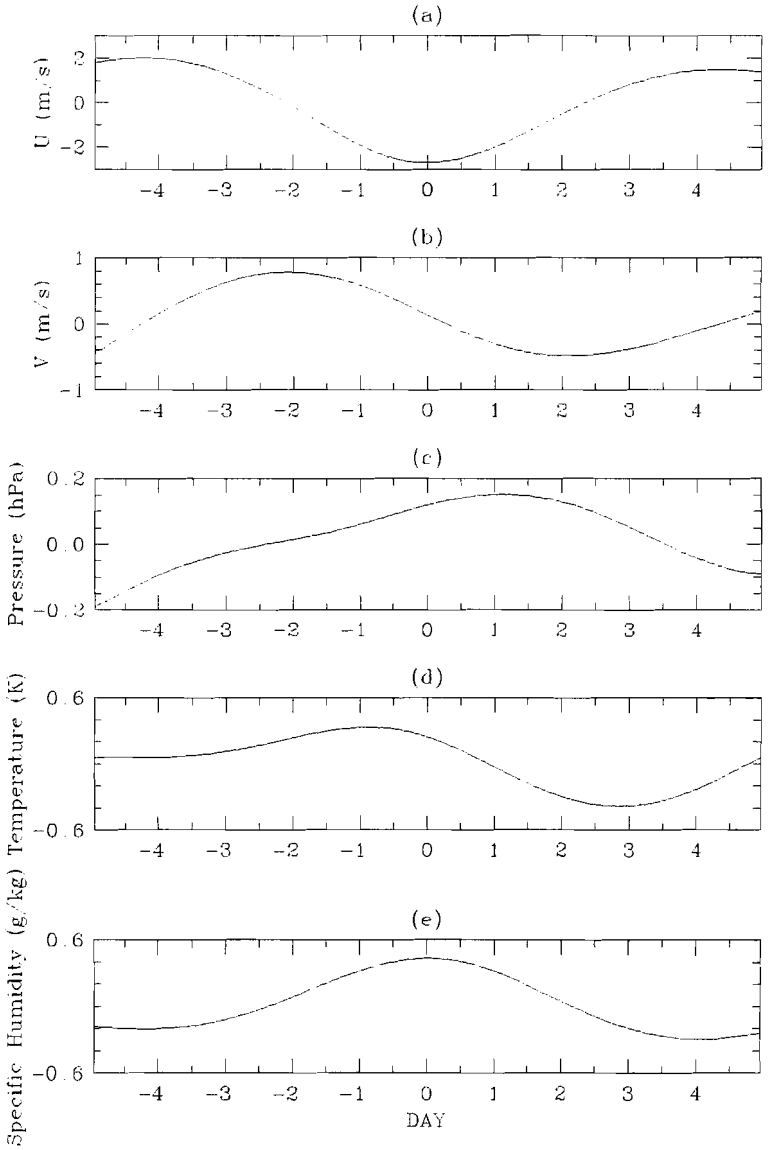

Figure 3.6: Composite time series of 7–13 day filtered (a) zonal wind by BLR averaged over 1–2 km height range, (b) meridional wind by BLR averaged over 1–2 km height range, (c) surface pressure, (d) surface temperature and (e) surface specific humidity. The horizontal axis represent day number from westerly wind minimum hour.

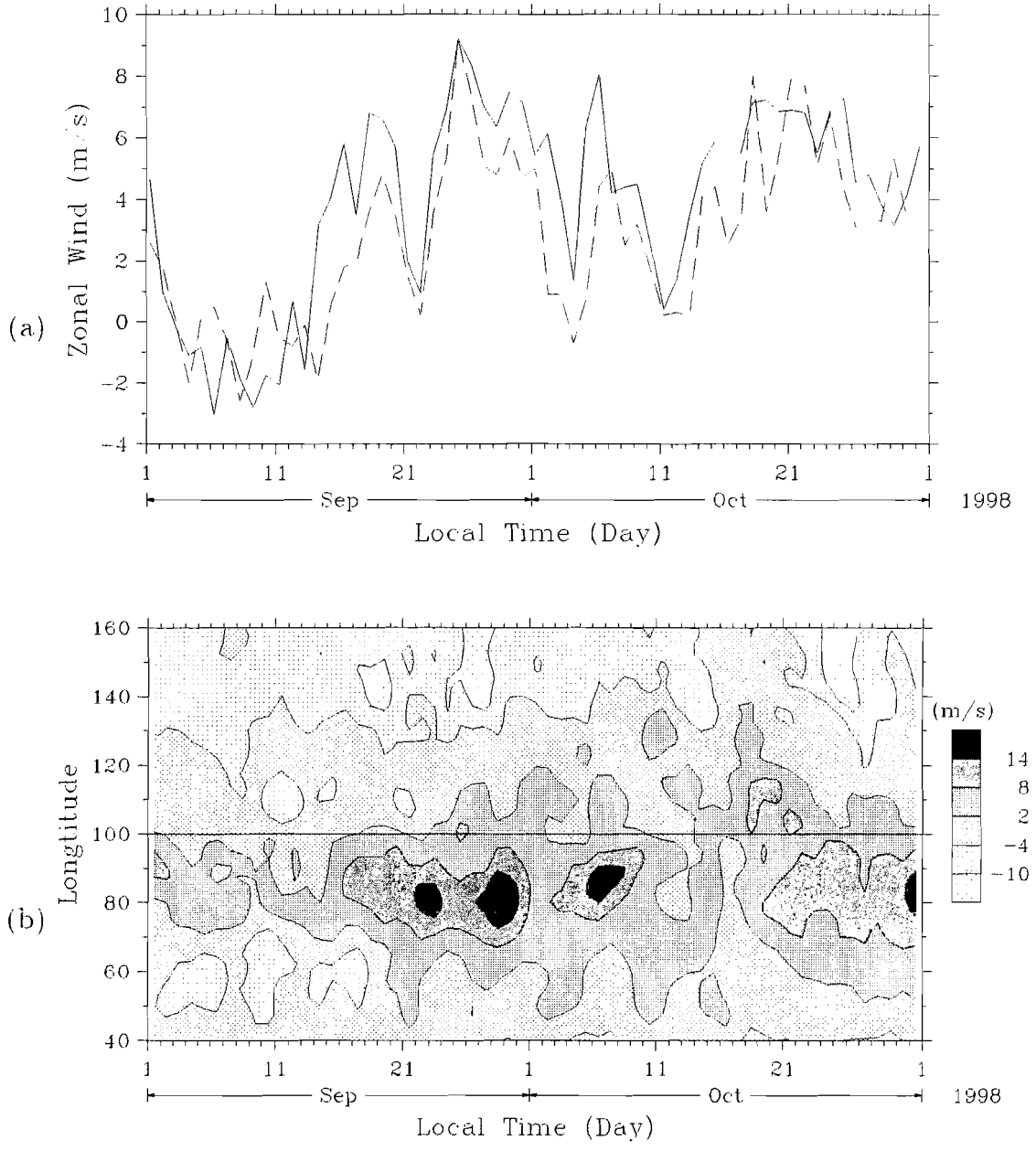

Figure 3.7: (a) Time series of zonal winds. Solid curve is BLR wind averaged every 60-min and over 0–1 km height range. Dotted curve shows NCEP 850hPa grid point data. (b) Time-longitude cross-section of zonal wind at 850hPa by NCEP.

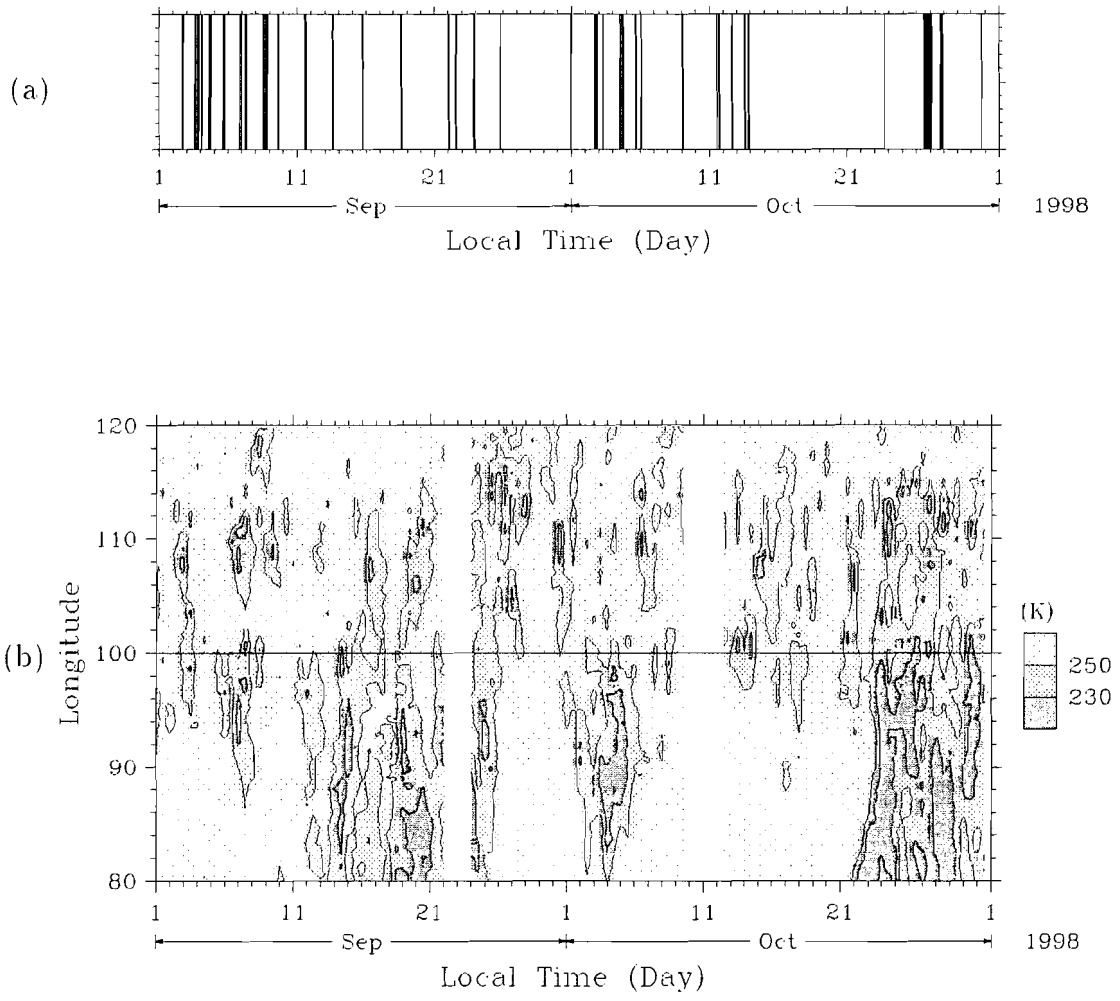

Figure 3.8: (a) Rainfall durations decided by BLR, same as in Fig. 4(b). (b) Time-longitude cross-section of 12-hourly GMS IR data averaged 2.6°S–2.6°N.

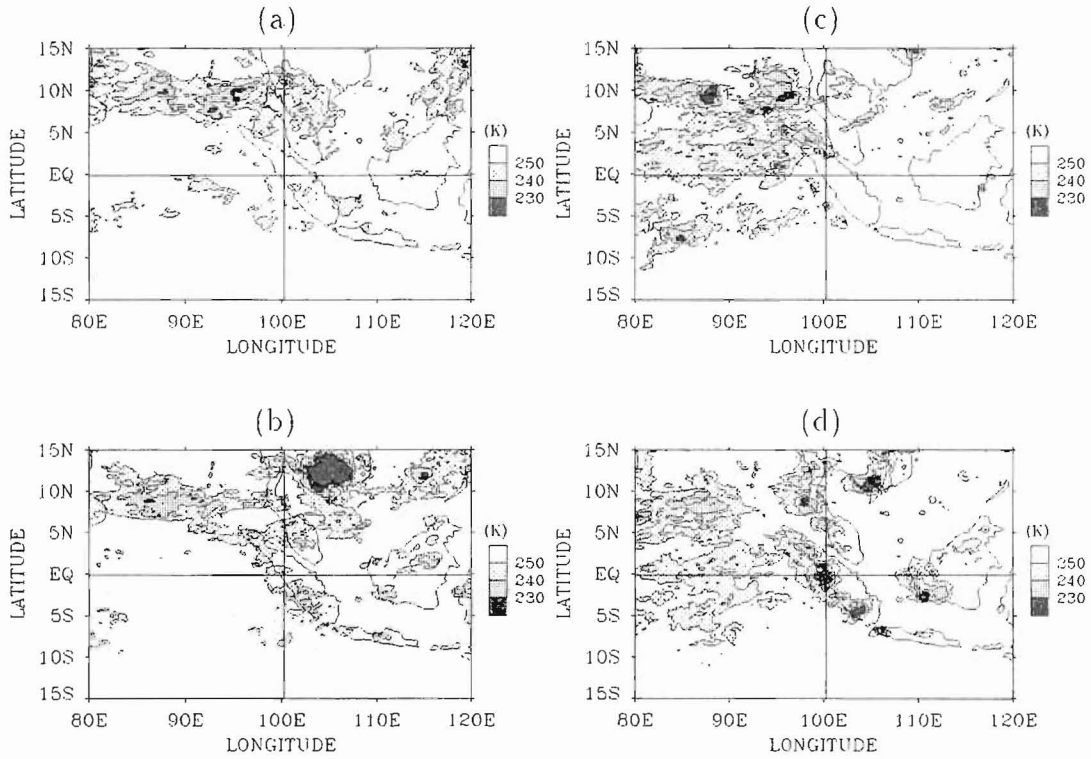

Figure 3.9: Composite maps of GMS T_{BB} data for the strong westerly periods [(a) 00 GMT and (b) 12 GMT] and for the weak westerly periods [(c) 00 GMT and (d) 12 GMT]. 00 GMT and 12 GMT correspond to 7 LST and 19 LST, respectively.

In the western side many tall clouds are dominant. Comparing the T_{BB} data [Fig. 3.8(b)] with the zonal wind field [Fig. 3.7(b)], the strong zonal wind fields are nearly coincident with the large-scale cloud disturbances (i.e., 11 September–10 October and 20–31 October), but the smaller scale variations have no good correlations with each other.

Figure 3.9 shows the composite of GMS T_{BB} data of 00 GMT and 12 GMT (corresponding to 7 LST and 19 LST, respectively) for the weak westerly periods (21–23 September, 2–4 October and 12–13 October; the data of 11 October was not used because of missing data) and the strong westerly period (16–18 September, 27–29 September and 6–8 October). There are only few clouds on Sumatera Island in the morning [see Figs. 3.9(a) and (c)], but many clouds are distributed on the mountain range which is located along the western coast in the evening [see Figs. 3.9(b) and (d)]. It implies that clouds on Sumatera Island have clear diurnal variation. Figure 11 also shows that the clouds on Sumatera Island are much more active during weak westerly periods [Fig. 3.9(d)] than strong westerly periods [Fig. 3.9(b)].

3.1.3 Discussions on the precipitation-wind relationship over Sumatera mountains

At Kototabang the precipitation occurred when the low-level westerly wind became weak (Figs. 3.1 and 3.2). Both the zonal wind and the precipitation varied with quasi-10-day periodicities during 15 September–15 October (Fig. 3.2), and the spectral analysis showed the clear peaks around 10 days for horizontal wind of the 1–2 km height range (Fig. 3.3). The surface meteorological variables had weak similar features with various phase-lags (Fig. 8), although they did not have clear spectral peaks near 10 days (Fig. 3.4).

Over the Indian Ocean (80–100°E) the cloud activities did not have clear 10-day periodicities (Fig. 3.8). However, the zonal wind (70–100°E) also varied with about 10-day periodicities (Fig. 3.7). In general, periodicities of the tropical cloud systems have been mainly discussed in the relationship to the theoretical equatorial waves. For example, Takayabu et al. (1996) found out a quasi-2 day mode from cloud activities by GMS, rainfall data by meteorological radars, rawinsondes, a UHF wind profiler and meteorological buoy data over the equatorial Pacific, and identified it with westward propagating inertio-gravity waves. Widiyatmi et al. (1999) found out a quasi-4 day mode in the Serpong BLR data, and GMS data in rainy seasons of Java Island, and considered that it may be mixed Rossby-gravity waves propagating westward. However, these are shorter than the time scales of periodicities found in this case study.

The quasi-10-day periodicities of wind and rainfall observed at Kototabang (Fig. 3.2) did not well correspond to the large-scale cloud disturbances over the Indian Ocean. It seems that the longitude 100°E was a zonal boundary for the cloud systems over the tropical Indian-Pacific Ocean regions (Fig. 3.8). The fact implies that effects of the mountain range blocked the large-scale Indian-Ocean disturbances. Some studies have already suggested the importance of the mountain range in Sumatera Island to the large-scale cloud activity. Nitta et al. (1992) analyzed the westerly wind burst, which is considered as one of the factors that cause El Niño events, affected by Sumatera Island. It is also known that ISO is sometimes depressed near 100°E (e.g., Murakami and Matsumoto 1994).

The local-scale cloud systems along the mountain range of Sumatera in Figure 3.9(d) are considered as the cause of precipitations with the quasi-10-day periodicities at Kototabang. The cloud systems were active in the evening. The obvious diurnal variations also appear commonly in Figures 3.3(b), 3.4 and 3.5. Nitta and Sekine (1994) showed from GMS IR data that diurnal variations are striking in cloud activities in/around the Indonesian maritime continent. Diurnal variations of rainfall characteristics in/around Sumatera Island have been suggested by Oki and Musiake (1994) for Malaysia, and by Hamada et al. (2002) for Indonesia. The geographical condition and the cloud distributions imply that the local-scale cloud systems had occurred by the convergence of sea breezes from the Indian Ocean and from the Strait of Malacca, or valley breezes.

Comparison between Figure 3.8(b) and (d) represent that the local-scale cloud systems had suppressed during the strong westerly periods. It is generally thought that local circulations are dominant under weak background winds. The development of the local-scale cloud systems themselves may have been controlled by the strength of the background wind.

3.2 Other results during September–October 1998

A correlation between precipitation at Kototabang and zonal wind was found and a plausible mechanism, the strong background wind suppress the development of local cloud systems, were suggested in Section 3.1. The zonal wind varied with quasi-10-day periodicities and had the clear spectral peak around 10 days(Figs. 3.2 and 3.3). In this Section, the causes of the quasi-10-day periodicities are discussed.

It is known that two types of equatorial waves have periodicities around 10 days. One is equatorial Kelvin waves which propagate eastward, and another is equatorial Rossby waves which propagate westward. The equatorial Kelvin waves have been observed mainly in the upper troposphere above Indonesia (Tsuda *et al.*, 1994; Fujiwara et al., 1998) and over southeast Asia and western Pacific (e.g., Nishi and Sumi, 1995). The existence of equatorial Rossby waves are indicated by satellite cloudiness data(Zangvil, 1975; Takayabu, 1994; Wheeler and Kiladis, 1999). Kiladis and Wheeler (1995) was found equatorial Rossby wave in the operational analysis data and discussed the structure of the wave.

Figure 3.10(a) is time series of zonal wind of NCEP reanalysis data at 850hPa (dotted line) and BLR data averaged 1–2 km height ranges (solid line). The both lines are coincident with each other, then we judged to utilize NCEP reanalysis data.

Figures 3.10(b) and (c) are time-height cross-sections at 850hPa of zonal wind anomaly and geopotential height anomaly from two months average. In zonal wind field, the westerly wind anomaly appear in 80–100°E on September 19 and propagate eastward with a phase spead of 5 m/s. More smaller disturbances which propagate westward about 10-day periodicity are also appear in this disturbance. The quasi-10-day disturbances can be seen more clearly in the geopotential height anomaly. The westerly anomaly corresponds to low pressure and the easterly anomaly corresponds to high pressure.

Figure 3.11(b) and (c) are horizontal distributions of 850hPa winds and geopotential height during the strong westerly periods at Kototabang. These are 7–13 band pass filtered. Low pressure anomalies appear in both side of equator and they bring the strong westerly wind near the equator. The structure of the disturbances is similar to that of theoretical n=1 equatorial Rossby wave (see Fig. 3.11(a)). The features of the quasi-10-day equatorial Rossby wave are listed in Table 3.1. The equivalent depth and the vertical wave length are estimated by Longget and Higgins (1968). It was agreed by the dispersion relation.

Figure 3.10 showed that the westward propagating zonal wind anomalies having around 10 day periodicities, which is clear only into the eastward propagating ISO, may contribute to the zonal wind variation observed at Kototabang. The horizontal structures of the wave and the dispersion relation suggest that the waves are identified as n=1 equatorial Rossby waves. There are a possibility that the large-scale convergence by the waves affect the precipitations at Kototabang. But the main convergence regions of the n=1 equatorial Rossby wave (Fig. 3.11(a))are away from the equator, then it might be difficult to consider that direct effect of the rainfall at Kototabang.

At the end of this section we recall Fig. 3.1. In the equivalent potential temperature field remarkable low value appeared during strong westerly periods. Figure 3.12 is a time-height cross-section of specific humidity anomaly during 27 September–7 October 1998. Obvious low humidity is seen during 5–7 October, which corresponds to low equivalent potential temperature. But before 2 October, which is another period of low equivalent potential temperature,

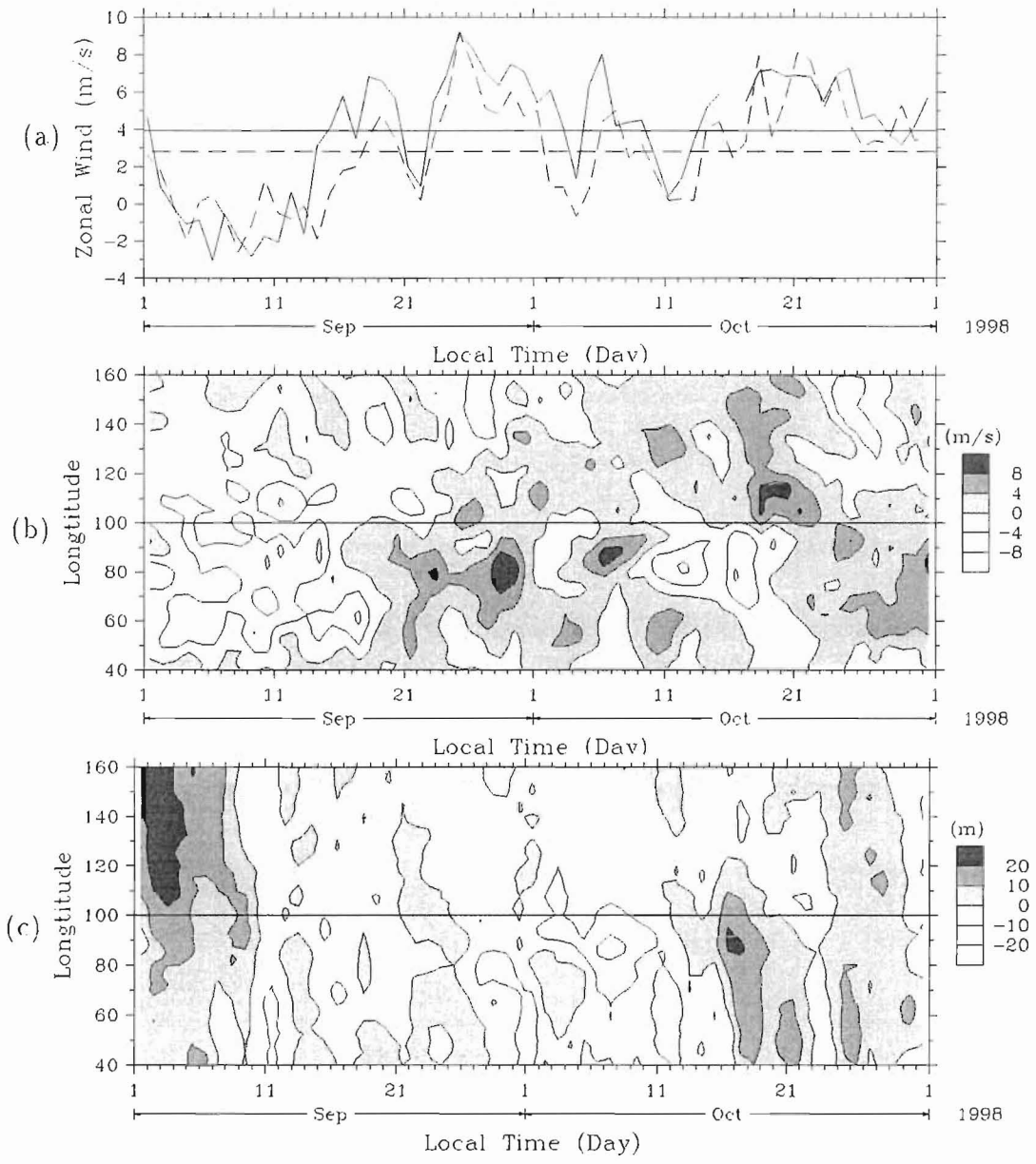

Figure 3.10: (a) Time series of zonal wind. Same as Figure 3.7(a). Lower two figures are time-longitude cross-sections of (b) anomalous zonal wind at 850 hPa and (c) anomalous geopotential height at 850 hPa from two months average.

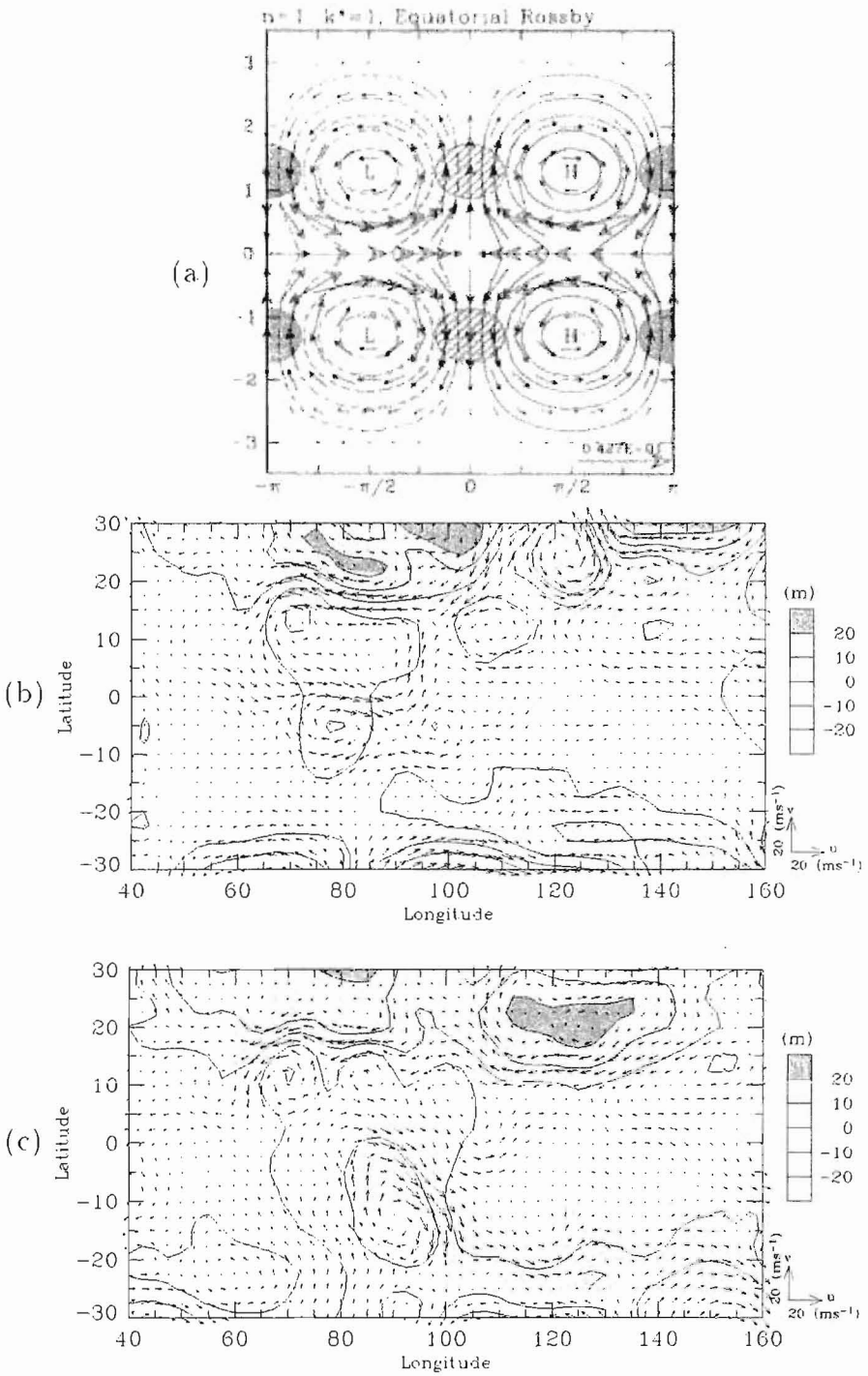

Figure 3.11: (a) The theoretical n=1 equatorial Rossby wave solution to the linear shallow water equations on an equatorial beta plane (Matsuno 1966) for a nondimensional zonal wavenumber 1. Hatching represent convergence and shading represent divergence (drawn by Wheeler et al., 2000). Composite maps of horizontal winds(arrows) and geopotential height(contour) at 850 hPa during (b) 27–29 September and (c) 6–8 October 1998.

Table 3.1: Features of the observed quasi-10-day equatorial Rossby wave

period	~10 days
phase speed	~10 m/s
wave number	4 ~ 5
wave length	~9000 km
equivalent depth	140 ~ 190 m
vertical wave length	11 ~ 13 km

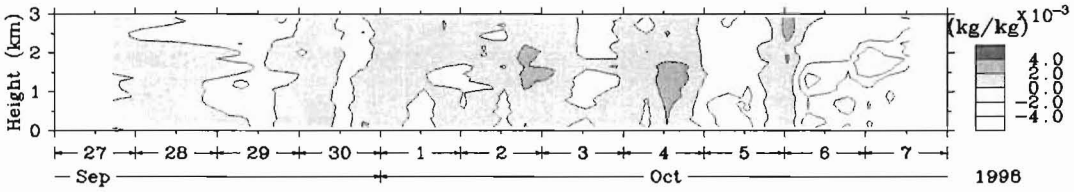

Figure 3.12: Time-height cross-section of specific humidity during 27 September–7 October 1998.

decrease of humidity is unclear. Such a correspondance between low equivalent potential temperature and low humidity had been observed during May–June 2001, which is described in next section.

3.3 Case study 2: May–June 2001

In the IOP during May–June 2001, the similar relations between westerly wind and precipitation discussed in Section 3.1 were observed. this period corresponds to the transition season from rainy season to dry season. Similarities and differences with the results appeared in Case study 1 are discussed.

3.3.1 Observational results

Figure 3.13 shows the results of IOP during 17 May–12 June 2001. Figure 3.13(b) is a time series of daily rainfall amount observed by raingauge (resolution is 0.2 mm). time-height cross-sections of zonal wind(Fig. 3.13) and the equivalent potential temperature 3.13 for the analysis period observed by rawinsondes. Many rainfalls occurred during June 1–7. Though the westerly wind in the lower troposphere was weak during the period, strong westerly more than 10 m/s appeared during May 28–29 and June 7–9 at the height of 1–4 km with a interval of about 10 days. The rainfalls did not occur during 29–31 May and 8–12 June after appearance of strong westerly wind. The lower atmosphere became dry over one day for several days after the appearance of strong westerly wind during May 29–30 and June 8–12, although the diurnal variation of humidity was remarkable during May 17–21 and May 31–June 7.

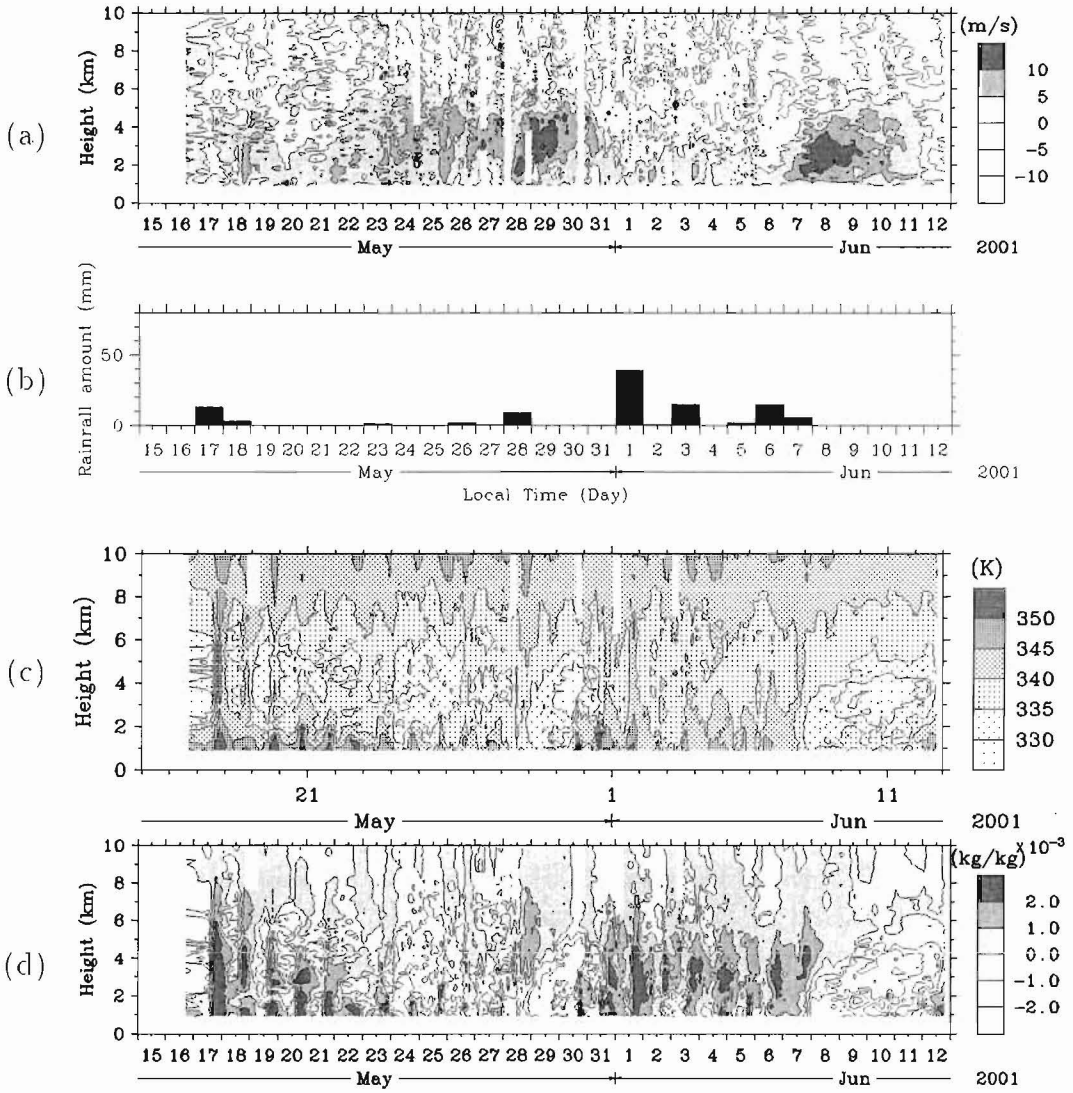

Figure 3.13: Results of the intensive observation period during 17 May–12 June 2001. Time-height cross-section of (a) zonal wind, (c) the equivalent potential temperature and (d) the specific humidity observed by rawinsondes. (d) Time series of daily averaged rainfall.

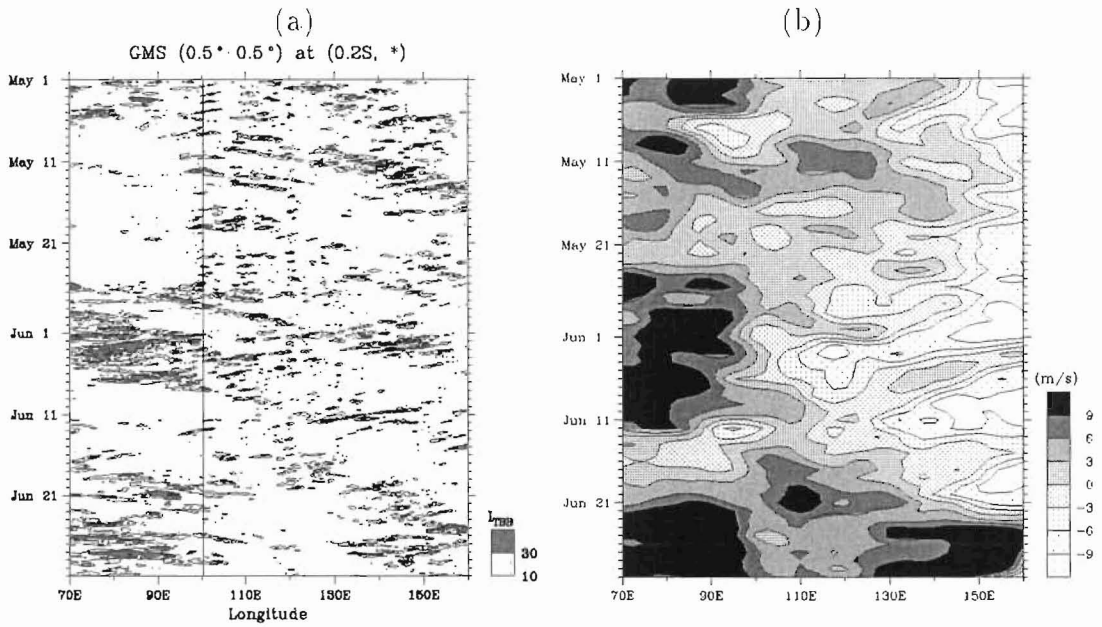

Figure 3.14: Time-longitude cross sections of (a) GMS T_{BB} data along 0.2°S and (b) NCEP 700hPa zonal wind along equator are shown during 1 May–30 June 2001

3.3.2 Comparisons with horizontal distributions

Figure 3.14 are the time-longitude cross sections of (a) GMS T_{BB} data along 0.2°S and (b) NCEP 700hPa zonal wind along equator during 1 May–30 June 2001. GMS data are averaged over the square of 0.5°, but the interval of NCEP grid point data is 2.5°. In GMS data only higher clouds which are correspond to the cloud top temperatures less than 240K are shown.

In this period the large cloud disturbance corresponding to ISO have propagated eastward since 25 May and the strong westerly have appeared at the same time on the equatorial Indian Ocean. However, the high clouds have become sparsely and seemed to be weakened after passing through Sumatera Island. The strong westerly also have remarkably weaken at the east of Sumatera. The eastward propagating cloud systems which horizontal scales are several hundreds kilometers have passed through Kototabang on 28 May and 7 June 2002 in the afternoon. These times correspond to the beginning of more than 10 m/s westerly at Kototabang. The eastward moving westerlies of 3–6 m/s seem to follow the clouds systems. After the passage of the clouds systems, the large regions over several thousands kilometers are lack of high clouds and this periods correspond to the dry events in lower troposphere at Kototabang.

3.3.3 Discussions

On the intensive observation during May–June 2001 similar relationship between low level westerly and precipitations were obtained. During strong westerly periods, low level drying were analyzed. There were a little lag between the beginning of strong westerly and drying, and drying continued several days even if the westerly became weak. The precipitations did not

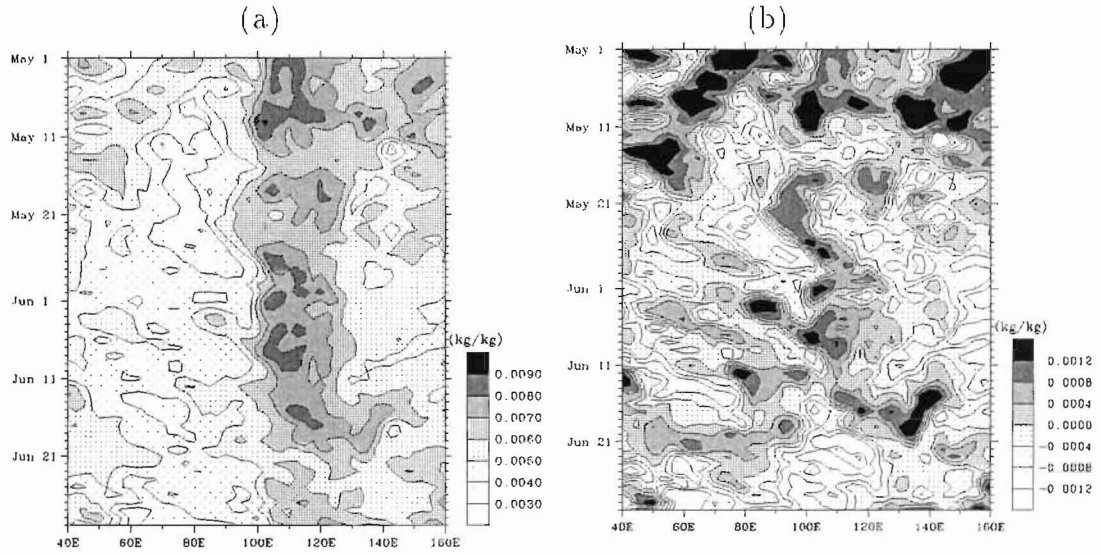

Figure 3.15: Time-longitude cross sections of (a) specific humidity and (b) its anomaly from two month average along equator are shown during 1 May–30 June 2001

occur during low level drying. The horizontal structure of GMS T_{BB} data and NCEP zonal wind at 700hPa indicated that the eastward propagating large scale disturbance appeared during this IOP. The strong westerly events occurred when the strong westerly following the large cloud disturbances blowed in the equatorial Indian Ocean. The large cloud disturbances and the strong westerly became weakened after passing through Sumatera Island. The appearance of strong winds observed at Kototabang were correspond to the eastward propagation of the cloud systems which scales are several hundreds kilometers. After passing the cloud systems, the high clouds over several thousands kilometers were absence for several days. It is suggested that the cloud activities over large regions are suppressed. It is considered that the local scale cloud systems, which usually develop in the afternoon, are suppressed at Kototabang.

The context of this chapter has been published as Renggono *et al.*(2001) and Murata *et al.*(2002).

Chapter 4

Statistical study

In Section 4, the relationship between low level westerly and precipitation at Kototabang is discussed by utilizing longer data during August 1999–April 2002. In Section 4.1 features of 700 hPa wind and precipitations and differences of precipitation percentage and precipitation types between weak and strong westerly are discussed. In Section 4.2 diurnal variations of convective activities for weak and strong westerlies are discussed. Relations with seasonal variation and intraseasonal variation are argued in Section 4.3. Discussions throughout this chapter and the lifting effects of mountainous region of Sumatera on the convections off the west coast of Sumatera described in Section 4.4.

4.1 Relationship between zonal wind and precipitation

The correlation between westerly and precipitation suggested in Chapter 3 is confirmed statistically. 700hPa NCEP zonal winds at nearest grid point (0°100°E) of daily averaged substituted for BLR because of insufficient amount of BLR data. The both values and variations are good coincident with each other, then it is expected that the same results will be lead by use of NCEP data. Rainfalls observed by rain gauge, which volume resolution is 0.2 mm, and total solar radiation observed by pyranometer, they are attached automatic weather station at Kototabang, are analyzed.

Figure 4.1 (a) is a scatter plot of zonal-meridional wind distribution. A vector from origin to each point shows wind direction, which upward direction on a parallel with vertical axis corresponds to northward wind or southerly wind. A distance between the origin and each point represents wind speed. The average wind was north-westerly wind with 2.63 m/s westerly component and 0.96 m/s northerly component. Standard deviations of each component are 4.02 m/s for zonal wind and 2.43 m/s for meridional wind. It corresponds to climatological analysis, which westerly wind is dominant in both summer and winter seasons in low troposphere (Matsumoto, 1992). Strong wind speeds tended to occur in westerly winds. It is known that the strong westerly anomalies appear following to ISO in the equatorial eastern Indian Ocean (e.g., Nitta *et al.* 1992).

In this analysis we investigate only zonal wind component. Figure 4.1 (b) shows frequency distributions of zonal wind component. Thin solid and dashed lines of (b) represent that for rainy days and no rainy days, respectively. Thick solid line is for total cases, that is, a

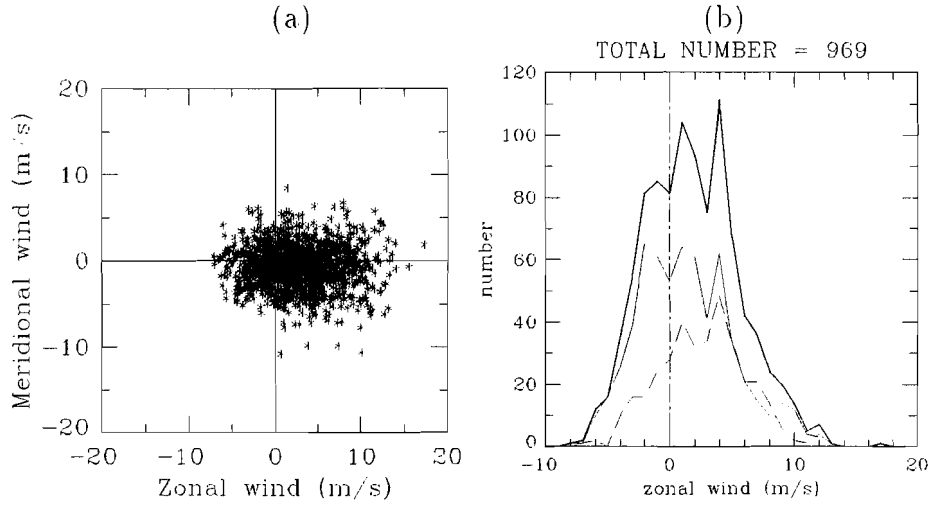

Figure 4.1: General feature of 700 hPa wind. (a) A scatter plot of zonal-meridional wind distribution, and (b) A distribution of frequency of zonal wind in the analysis period. Thin solid and dashed lines of (b) represent that for rainy days and no rainy days, respectively. Thick solid line is for total cases, that is, a sum of rainy and no rainy days.

sum of rainy and no rainy days. The averages (standard deviations) of distributions are 1.76 (3.83) m/s for rainy days and 3.09 (3.49) m/s for no rainy days, respectively. To simplify the discussion, zonal wind speed are considered and the differences between westerlies and easterlies are left as future works. Because easterlies are weak and much less than westerlies, results could be interpreted as differences of westerly strength.

Figure 4.2 (a) is a histogram of rates of each 1 m/s zonal wind speed bands for total days and Fig. 4.2 (b) represent rates occupied by westerly wind in each zonal wind speed band. Rate of westerly wind increases when wind speed is strong, and the rate of westerly exceed 80 percent for days of more than 4 m/s wind speed. In Figure 4.2 (a) thin solid line is a histogram for rainy days and thin dashed line is that for no rainy days. Thick solid line is sum of rainy and no rainy days. 63 percent of total days are rainy days. The days of less than 3 m/s wind speed occupy around 50 percent of total days. The rate of rainy days decrease rapidly as wind speed becomes strong. No rainy days are kept around 5 percent of total days in each wind bands when wind speed is less than 5 m/s. The rate of no rainy days exceed that of rainy days in 6–9 m/s wind speeds.

Figure 4.3 (a) shows rates of rainfall amounts in each wind speed bands for total rainfall amount. 60 percent of total rainfalls occur in days of less than 3 m/s wind speed. A solid line (dashed line) of Fig. 4.3 (b) represents rates of rainy days when wind speeds are lower (higher) than the x-axis values. the rates are calculated for more than 50 cases. A thin solid line and two dot-dashed lines represent rate of rainy days for total cases and 95.4 % confidence interval under an assumption that rate of rainy days do not depend on wind speed,and rates of rainy days are same as that for total cases.

The rate of rainy days get maximum for cases of less than 2 m/s wind speed and get minimum for cases of more than 6 m/s wind speed. The fact that these extreme values are out

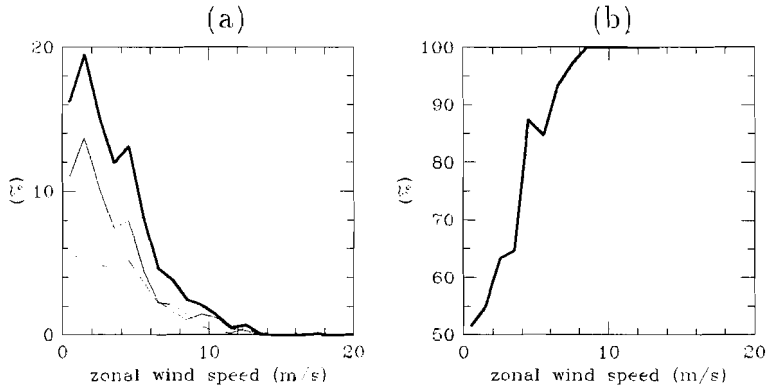

Figure 4.2: (a) A histogram of occurrence rate in each 1 m/s zonal wind speed bands for total days. Thin solid line is that for rainy days and thin dashed line is that for no rainy days. Thick solid line is sum of rainy and no rainy days. (b) Rate of westerly wind in each 1 m/s zonal wind speed band.

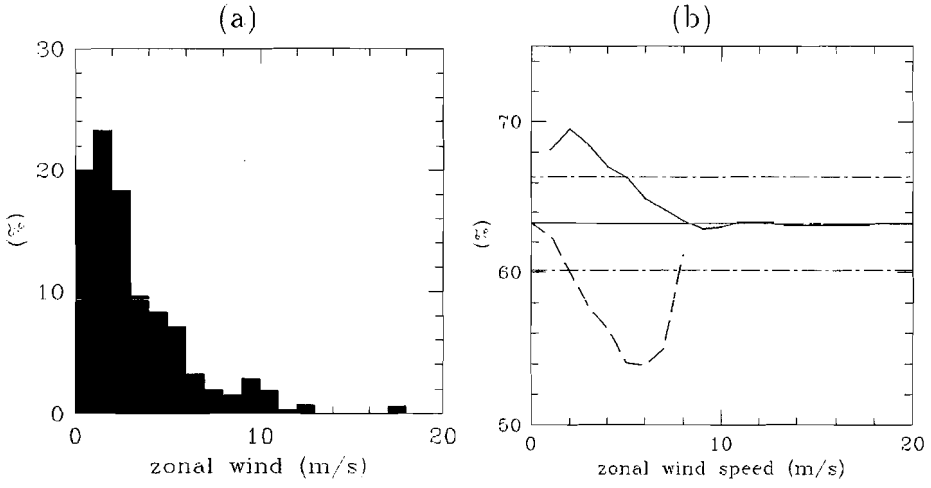

Figure 4.3: (a) rates of rainfall amount in each wind speed bands for total rainfall amount during the analysis period. (b) A solid line represent rate of rainy days when wind speeds are lower than the x-axis values. A dashed line represent rate of rainy days when wind speed are higher than the x-axis values. Thin solid line shows rate of rainy days for total cases. these rates are calculated for more than 50 cases. Two doted-dashed horizontal lines represent 95.4 % confidence interval under an assumption that rate of rainy days do not depend on wind speed and rate of rainy days are same as that for total cases.

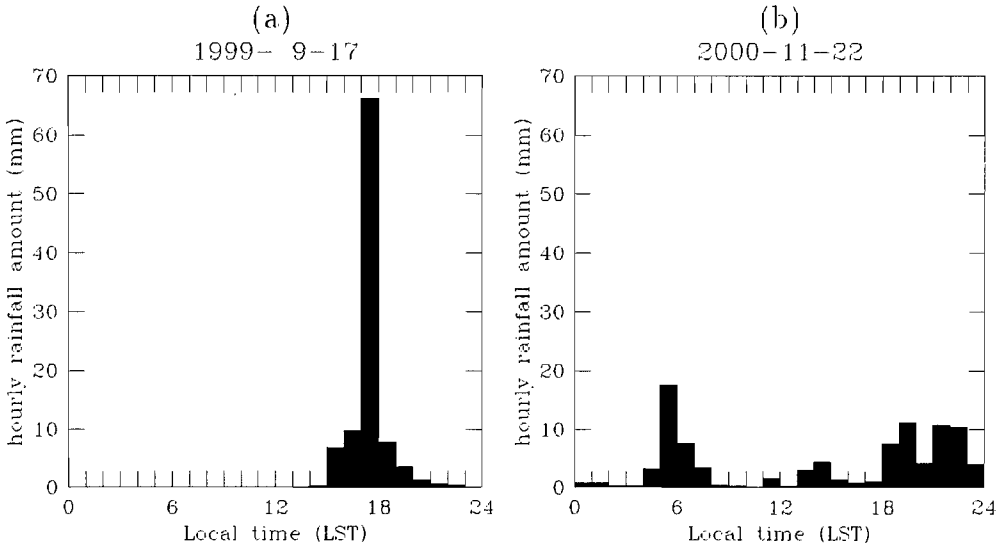

Figure 4.4: Diurnal variations of the days of each maximum daily rainfalls for for (a) group A and (b) group B.

of 95.4 % confidence interval implies that the rates of rainy days depend on wind speed and they are high (low) under weak (strong) 700 hPa wind speeds, based on maximum likelihood method.

4.2 Difference by westerly strength

In this section features of precipitating cloud systems under weak and strong 700 hPa wind are examined. Conditions are divided by zonal wind speed of 5 m/s, which corresponds to around a minimum threshold of rainfall probability for strong winds. The days of less than 5 m/s and that more than 5 m/s are classified into group A and group B, respectively.

The dominant cloud systems in each group are considered. We analyze only one station data. Generally, scales of cloud systems are several ten to hundreds kilometers and probability that cloud system and its center of convection pass through above Kototabang is much low. Then the maximum rainfall events are firstly analyzed to know the typical features of cloud systems, because it might correspond to the case of center of cloud systems. During analysis periods, Kototabang experienced two cases of strong diurnal rainfall amounts more than 90. mm, but westerly wind speed was different. Figure 4.4 shows diurnal variation of rainfalls on these extreme cases. Figure 4.4(a) represents a case of group A or weak wind days, which is 1.2 m/s. Diurnal rainfall amount was 96.6 mm. Rainfall amount of 66.2 mm (around 70% of daily rainfall amount) occurred during one hour on 17 LST. Figure 4.4(b) shows a case of group B or strong wind days, which is 5.1 m/s. Diurnal rainfall amount was 95.0 mm, which is comparable to former case. However, the diurnal variation of rainfall is completely different. The maximum hourly rainfall is 17.6 mm, which is much less than former case and which occurred on 5 LST. The second peak appears around 19–23 LST and relatively small peak exists on 14 LST. A

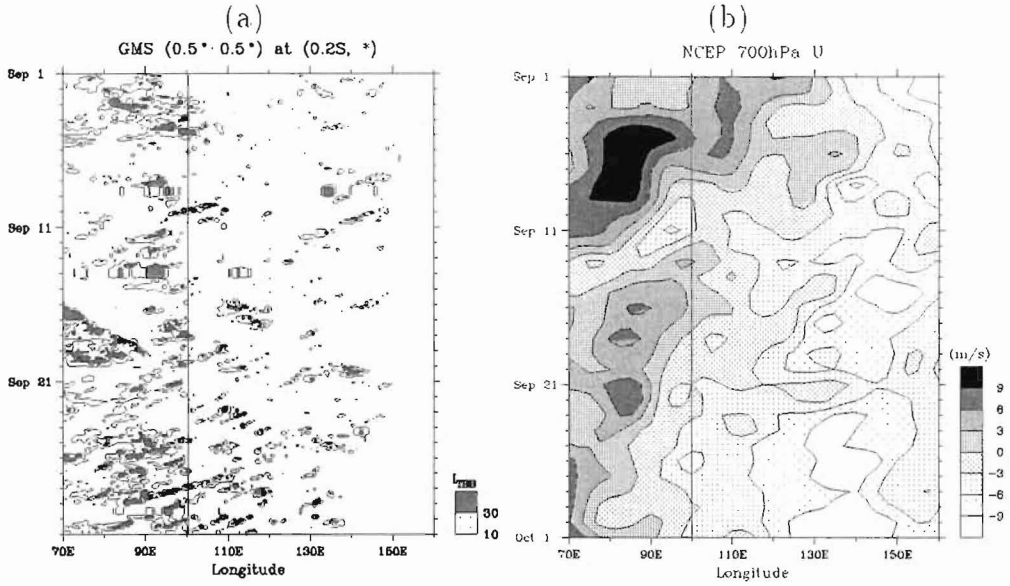

Figure 4.5: Time-longitude cross sections of GMS T_{BB} and NCEP 700 hPa in September 1999. The day of maximum daily rainfall for for group A was occurred in this period.

review for peak times of diurnal rainfall variation by Fujibe (1999) describes that morning maxima tend to be pronounced for deeper cloud than shallower ones, and midnight maxima over land areas may be characteristic to long-lasting heavy precipitations.

Figures 4.5 and 4.6 represent time-longitude cross sections of GMS T_{BB} and NCEP 700 hPa for the days of each maximum daily rainfalls for group A and group B. In the case of group A, many active convections appears in the Indian Ocean between 70–100°E and some of them are organized. But the convection on 17 September along 100°E (location of Kototabang) does not seem to be organized. It develops in the afternoon between 98–100°E. Westerlies appears during the first week, but easterlies prevail during this month. The case of group B corresponded to the period when eastward propagating convective cloud system passed through 100°E on 21–22 November. The cloud systems begin to follow strong westerlies on 19 November, the strong westerly region passed Kototabang just after passage of propagation of cloud system.

Figure 4.7 and 4.8 represents that mean diurnal variations of frequency of rainfall for daily amount more than 30 mm and 0.2 mm, respectively. The distributions are normalized by daily rainfalls. The distribution of group A shows dominance of afternoon rainfalls. A little increase of morning rainfalls are indicated in case of low threshold (0.2 mm). The mean diurnal variation for more than 30 mm daily rainfalls indicate large afternoon rainfall maxima except for morning peak. This is different from case of maximum daily rainfall day. The distribution of mean diurnal variation for low threshold indicate dominant afternoon rainfall and rather similar to group A.

Figure 4.9 (a) shows rates of rainfall amounts in each wind speed bands for total rainfall amount. 60 percent of total rainfalls occur in days of less than 3 m/s wind speed, and most of cases have intense hourly rainfalls. Figure 4.9 (b) shows mean daily rainfalls in each wind

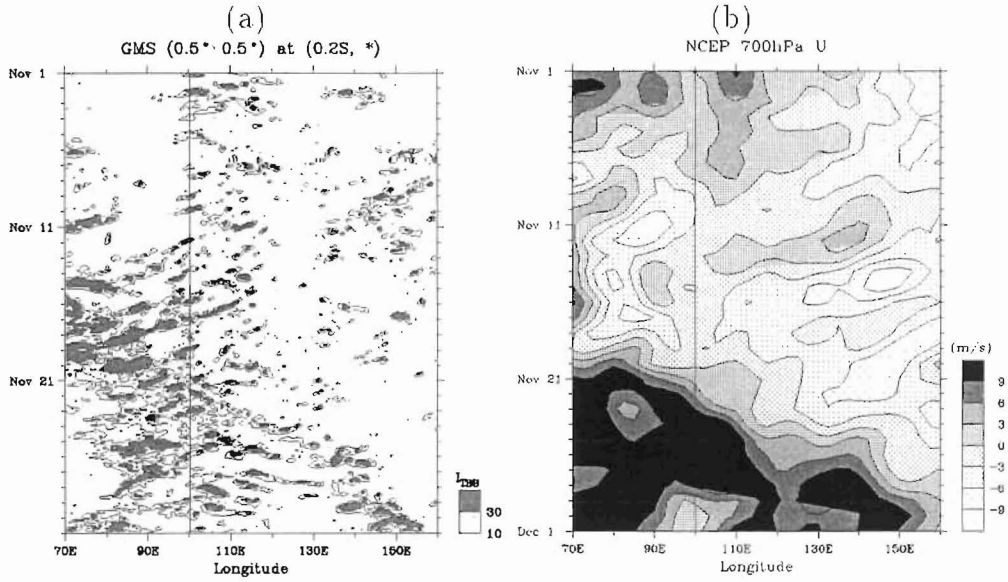

Figure 4.6: Time-longitude cross sections of GMS T_{BB} and NCEP 700 hPa in November 2000. The day of maximum daily rainfall for for group B was occurred in this period.

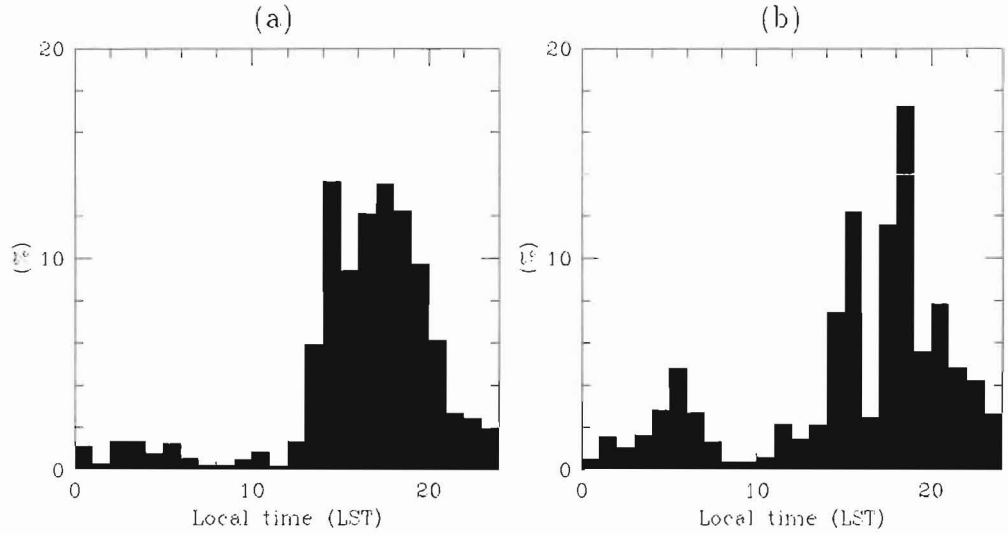

Figure 4.7: Mean diurnal variations of frequency of rainfall for (a) group A and (b) group B for more than 30 mm daily rainfall amount.

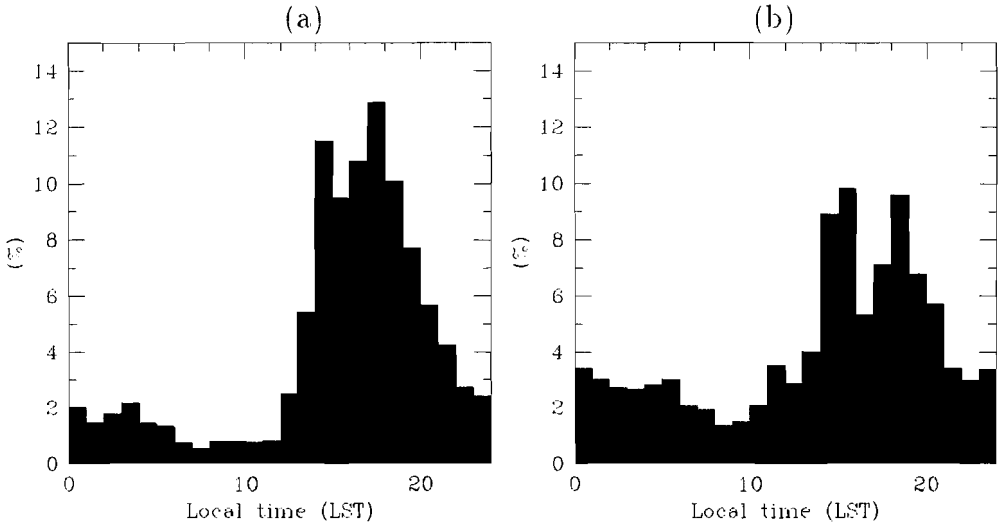

Figure 4.8: Mean diurnal variations of frequency of rainfall for (a) group A and (b) group B for more than 0.2 mm daily rainfall amount.

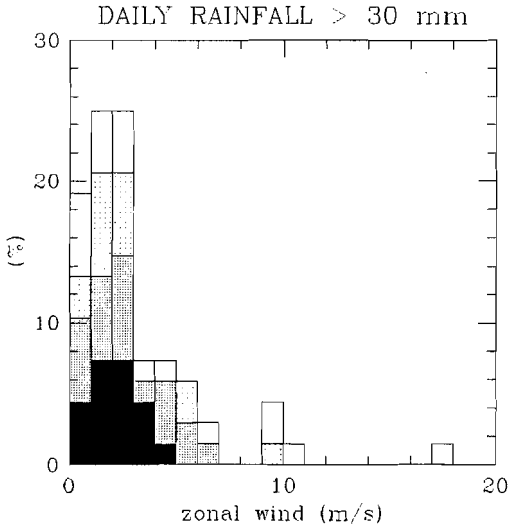

Figure 4.9: rates of rainfall for total days (68 cases) in which daily rainfalls are more than 30 mm. Three contours in this figure show rates of hourly maximum rainfalls more than 30 mm/h (black color), 20 mm/h (dark color) and 15 mm/h (light color), respectively.

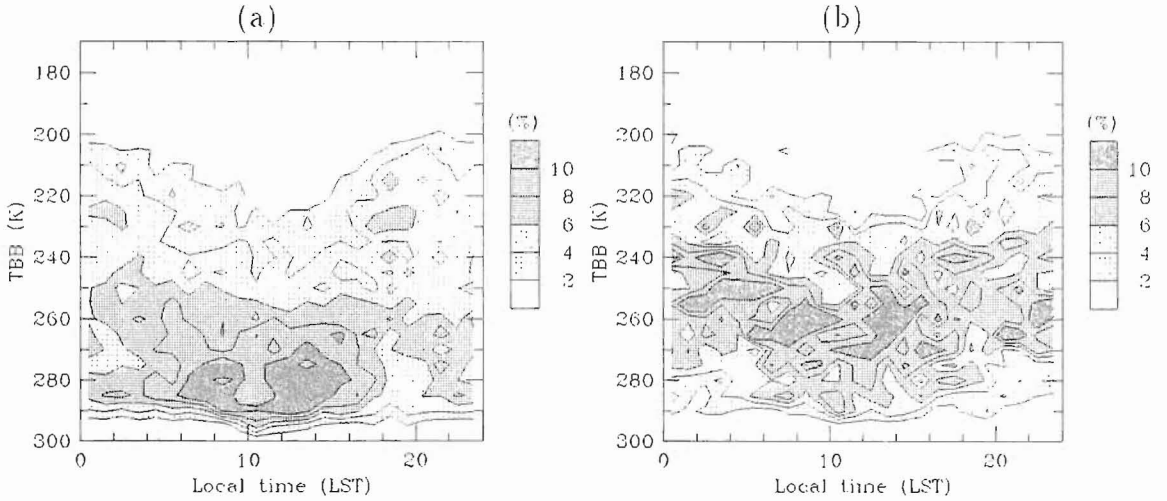

Figure 4.10: Diurnal variations of frequency of T_{BB} for (a) less than and (b) more than 5 m/s 700 hPa zonal wind speed. Contours are drawn by 5 K.

speed bands. A doted-dashed line shows 7.2 mm, which is mean daily rainfall for total days. Wind speed bands which have more than 10 cases are drawn. In 3–9 m/s wind speed bands daily rainfall amounts are lower than the mean value for total cases. Figure 4.9 (c) represents rates of rainfall for total days (68 cases) in which daily rainfalls are more than 30 mm. Three contours in this figure show rates of hourly maximum rainfalls more than 30 mm/h, 20 mm/h and 15 mm/h, respectively. The dark color shows strong hourly maximum rainfalls. The all rainy days observed more than 30 mm/h concentrate less than 5 m/s wind speed. 20 mm/h rainfalls occurred in the half of rainy days of less than 5 m/s wind speed. Figure 4.9 (d) shows mean total solar radiation for each wind speed bands. On less than 5 m/s wind speed solar radiations are steady and around 14 MJm^{-2}. From 5 m/s to 9 m/s mean total solar radiations decrease.

Figure 4.10 (a) shows occurrence frequency of T_{BB} for less than 5 m/s 700 hPa zonal wind speed. At 6–16 LST frequency more than 10% concentrate between 270–290 K, which correspond to surface level. During 16–20 LST occurrences of high T_{BB} around 280 K decrease and low T_{BB} less than 230 K increase. Occurrence frequency of 2% gradually increase from 12 LST. A little increase of high T_{BB} appear at 20 LST, and then, occurrences of low T_{BB} decrease during 0–11LST.

Figure 4.10 (b) is same as (a) but for more than 5 m/s 700 hPa zonal wind speed. High occurrence frequency more than 8 % appears around 240 K at 00Z, shift to high T_{BB} in the morning, and distribute around 250–270 K during 6–16 LST. Occurrence frequency of low T_{BB} less than 230 K increases during 16–20 LST. The differences between Figs. (a) and (b) is obvious in the daytime (6–16 LST). It is clear or it appears very low clouds in weak wind days (Fig. 4.10), but on strong wind days (Fig. 4.11) low clouds which correspond to T_{BB} around 260 K cover above Kototabang. The occurrence frequency of low T_{BB} less than 230 K is around 3% in Fig. 4.10, but around 4% in Fig. 4.11.

Figure 4.11 represent diurnal variation of T_{BB} occurrence frequency distributions on weak

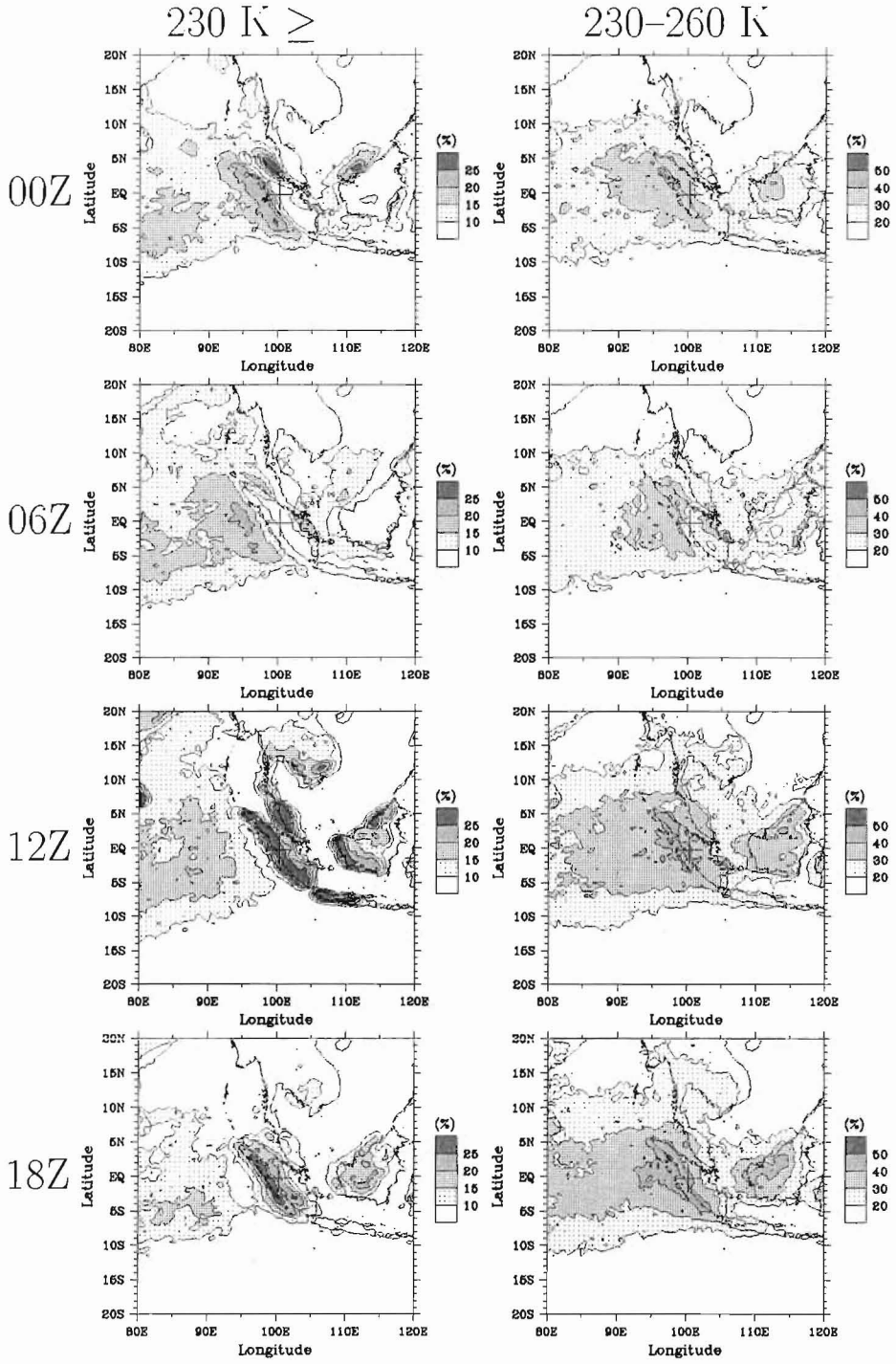

Figure 4.11: Composite diurnal variation of T_{BB} for weak wind rainy days. Right figures are occurrence frequency of T_{BB} less than 230 K, and left figures are same but 230–260 K at 00, 06, 12 and 18 UTC.

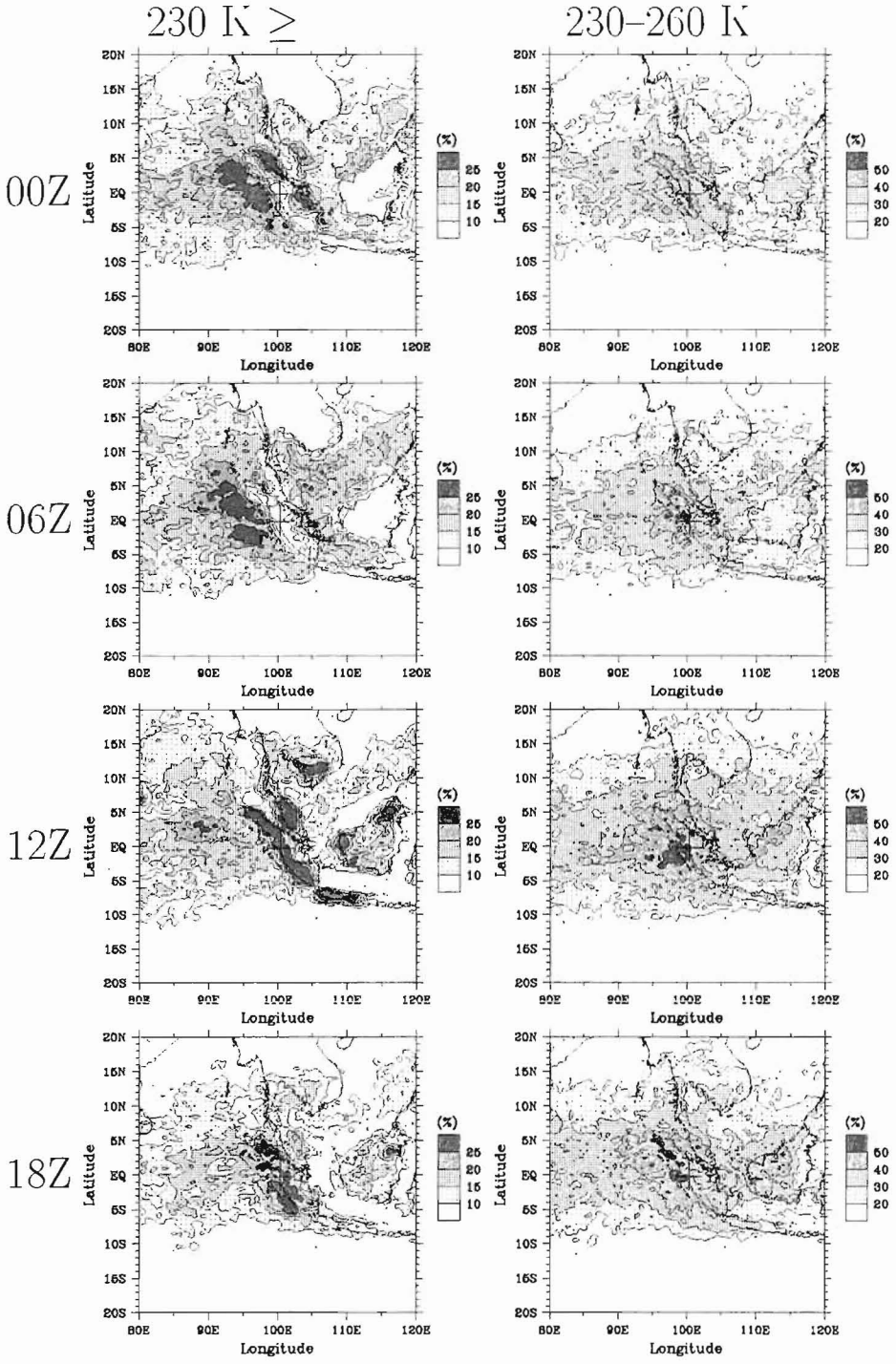

Figure 4.12: Same as previous figure but for strong wind rainy days.

Table 4.1: Features of weak and strong westerly

	group A	group B
zonal wind speed	less than 5m/s	more than 5m/s
total rainfall	76%	24%
maximum daily rainfall	96.6 mm	95.0 mm
mean daily rainfall	7.3 mm	6.5 mm
daily rainfall intensity ($\geq$ 30 mm/d)	83.8%	16.2%
hourly rainfall intensity ($\geq$ 30 mm/h)	100.%	0.%
solar radiation	14.4 MJm^2	11.6 MJm^2
morning/afternoon ratio	14.6 / 85.4	30.0 / 70.0

zonal wind days and on precipitating days at Kototabang. Right figures are drawn for T_{BB} less than 230 K, and left figures are drawn for 230–260 K. 00, 06, 12 and 18Z correspond to 07, 13, 19 and 01 LST at Kototabang. At 00Z more than 15% occurrence of active convections of less than 230 K is wide spread in eastern Indian Ocean, especially develop several hundreds kilometers off the west coast of Sumatera, Malacca Strait and off the northwest coast of Kalimantan(Borneo). The offshore convections move seaward to more several kilometers off with decreasing their top heights at 06Z. Convection in lands become active in western part of Sumatera, Java, western and northern Kalimantan, southern part of Malay Peninsula and southern part of Indo-China. At 18Z active convection appears just off the west coast of Sumatera. Convective active region of west coast of Sumatera seem to move westward systematically. T_{BB} occurrence of middle level clouds for 230–260 K increase on land regions in the late afternoon to midnight (12Z and 00Z). Figure 4.12 is same as Fig. 4.11 except for strong wind days. Compared to weak wind days, convections in the ocean in 10°N–10°S region are more active and occurrences of high clouds become maximum at 06Z. Chen and Houze (1997) pointed that diurnal variation of oceanic convection depended on threshold value and cloud coverage became maximum around 14 LST for 205–235 K. The diurnal variation is obvious and locations where convections tend to occur are almost same as that for weak zonal wind days. The amount of middle level clouds in strong zonal wind days is about 10 % larger than that in weak wind days.

Figures 4.13 and 4.14 show composite diurnal variations of T_{BB} horizontal distribution of no rainy days at Kototabang for weak and strong wind days, respectively. Compared to composite maps for rainy days (Figs. 4.11 and 4.12), convective activities over oceanic region are inactive for composite maps of no rainy days. In land regions clouds develop at 12Z over same regions as distributions of rainy days, except for the vicinity of Kototabang. It is interesting that convective activities over equatorial regions across over 3°S and 3°N are inactive (occurrence frequency of less than 230 K is less than 10%)in all four local time. Over the oceanic region of the east of Malaysia TBB occurrences of 230–260 K is less than 20%, besides low occurrences of less than 230 K. The occurrence of TBB less than 230 K is higher than that in strong wind days, but the occurrence of 230–260 K in same area is low, then these clouds are considered as not convective but high clouds.

Table 4.1 is summary of analyses for conditions of weak and strong westerly days. The most of rainfalls occur under weak westerly conditions. The strong intensity rainfalls tend to occur

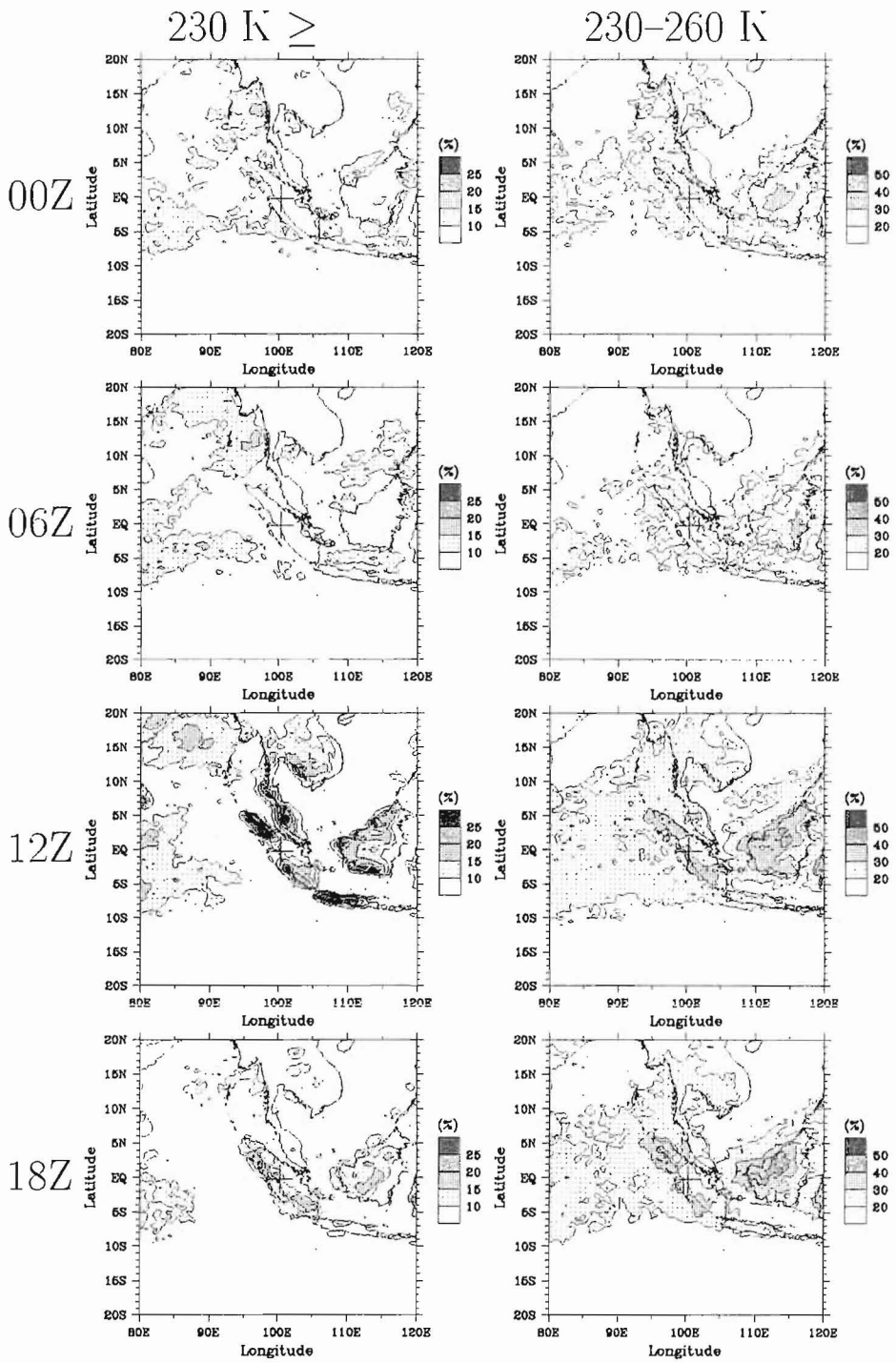

Figure 4.13: Composite diurnal variation of T_{BB} for weak wind no rainy days.

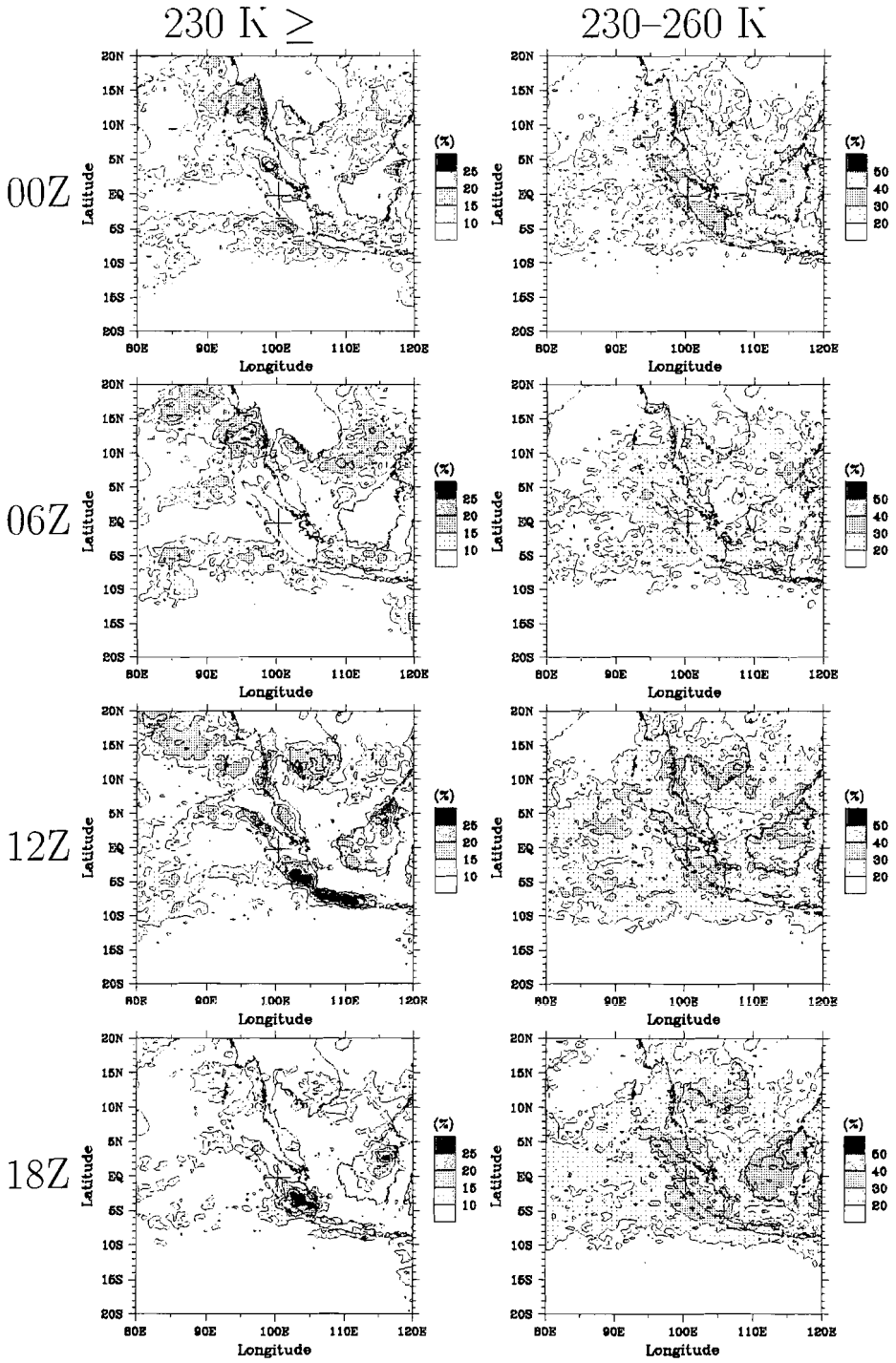

Figure 4.14: Same as previous figure except for strong wind no rainy days.

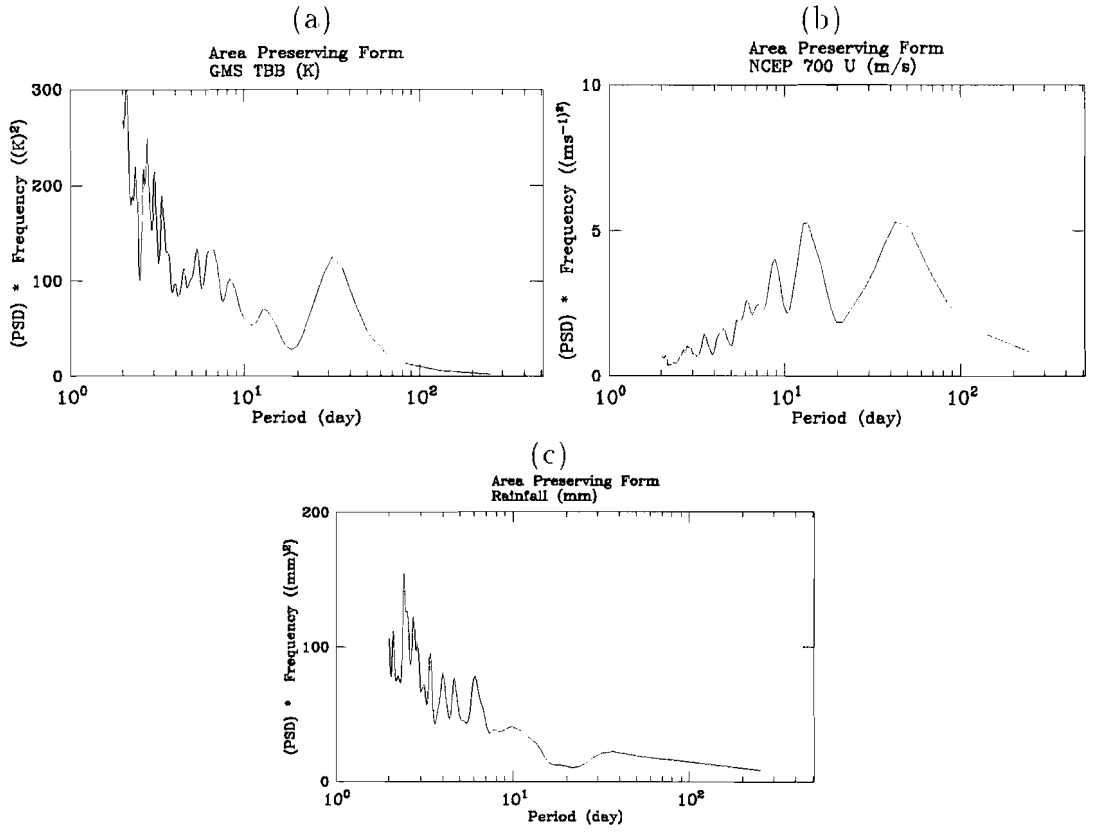

Figure 4.15: Spectral analyses of (a) GMS T_{BB} data at (0°, 100°E) averaged over 0.05°square, (b) NCEP 700 hPa zonal wind at (0°, 100°E) and (c) daily rainfall amount observed by rain gauge at Kototabang during 1 August 1999–30 April 2002 (lag=128).

in weak westerly days, which consistent with relative large solar radiations and high cloud top temperatures (which are near the surface temperature) in the daytime. The maximum daily rainfalls during analysis periods and mean daily rainfall amounts are similar with each other. The rainfalls generally occurred from diurnally developing local cloud systems which are develop along the mountainous region in the afternoon.

4.3 Effects of other variations

Figure 4.15 shows the results of spectral analysis. For GMS T_{BB} time series of one day mean 0.05° longitude-latitude square averaged data at (0°, 100°E) are utilized. T_{BB} and rainfall data have large high frequency perturbations within 10 days. Frequencies around 10 days and 30–50 days are detected in all three data.

Figure 4.16 shows 20–90 day bandpass filtered GMS T_{BB} and NCEP 700 hPa zonal wind time series. The time series utilized this analysis is same as that utilized in spectral analysis (Fig. 4.15). Solid lines and dashed lines show time series at (0°, 100°E) and at (0°, 90°E), respectively. Both time series of T_{BB} are similar with each other, but for zonal wind phase and amplitudes are sometimes quite different.

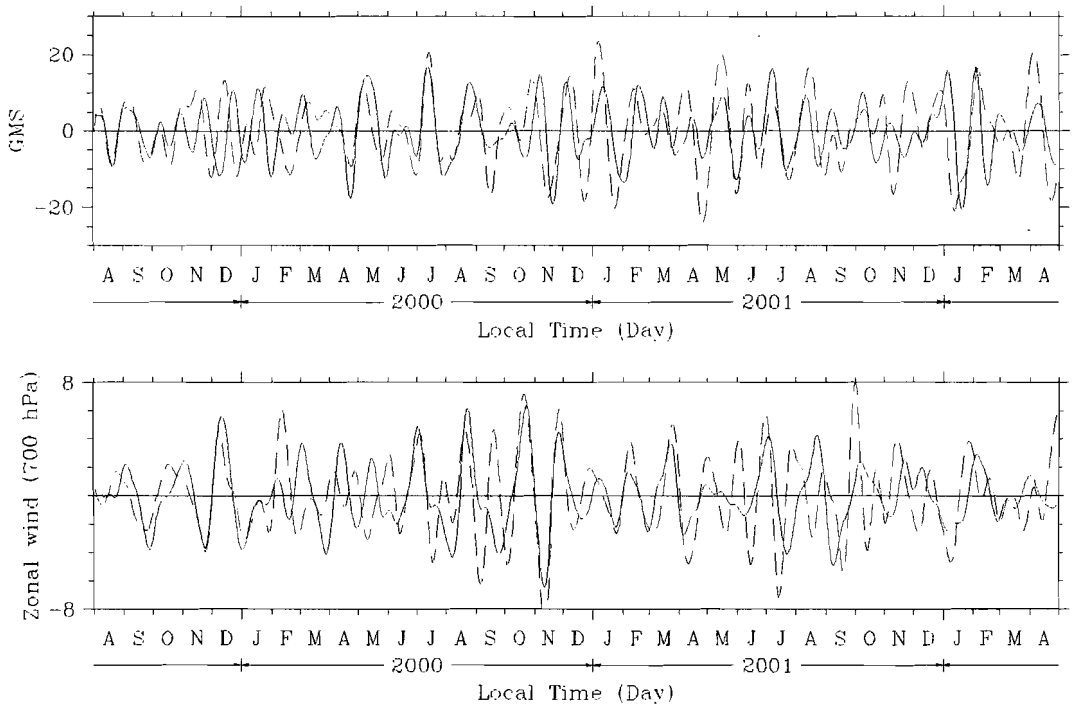

Figure 4.16: 20–90-day bandpass filtered GMS T_{BB} data in 0.05°square, and NCEP 700 hPa zonal wind. Solid and dashed curves represent variations at (100°E, 0°) and (90°E, 0°), respectively.

Table 4.2: Base days for composite analysis

1999	2000	2001	2002
Aug 20	Jan 15	Jan 25	Jan 13
Sep 25	Feb 21	Feb 26	Mar 2
Oct 21	Apr 24	Mar 26	Mar 20
Dec 2	May 26	Apr 27	Apr 24
Dec 29	Jul 1	Jun 1	
	Jul 28	Jun 25	
	Aug 9	Jul 25	
	Sep 17	Aug 31	
	Oct 19	Sep 18	
	Nov 17	Oct 21	
	Dec 24	Nov 11	
		Dec 11	

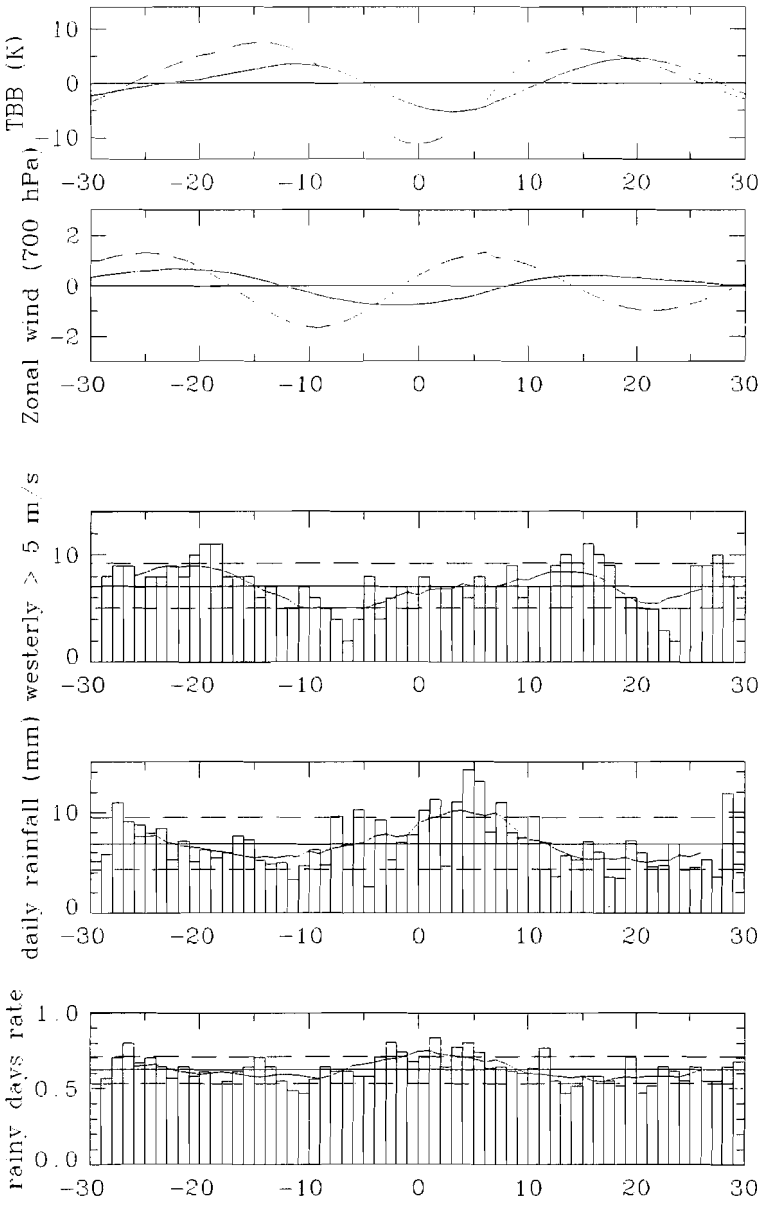

Figure 4.17: Composite variations of 20–90-day bandpass filtered (a) zonal wind and (b) GMS T_{BB} data for 90°E (dashed lines) and 100°E (solid lines). (c) Number of strong zonal winds more than 5 m/s for each phase. (d) Total rainfall amount for each phase. (e) Number of rainy days for each phase. Horizontal line represent days relative to base days. Base days are decided by T_{BB} minimum values at 80°E. Each horizontal line of (c), (d), (e) represent average values (solid line) and width of standard deviation (dashed line). Solid curves of (c), (d), (e) represent 9 days running mean.

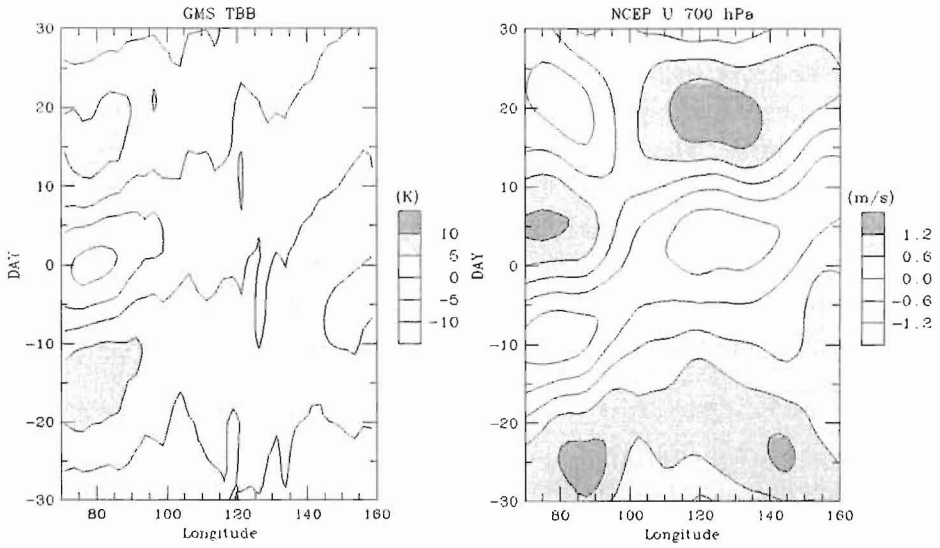

Figure 4.18: Time-longitude cross-sections for 20–90-day filtered GMS T_{BB} data and NCEP 700 hPa zonal wind. Time represents deviation from base days.

To analyze the relationship between intraseasonal oscillations and rainfalls and strong winds at Kototabang, Composite analysis are applied . 14 base days shown in Table 4.2 are selected as it takes minimum values of 20–90 bandpass filtered T_{BB} and amplitudes are more than 10 K Intraseasonal convective activities between 90°E and 100°E are nearly in phase. The phase of zonal wind at 90°E is around 10 days earlier than that of T_{BB} and after 5 days the maximum convections westerly anomaly reach a peak. The phase of zonal wind at 100°E have minimum at -8 day and maximum around +13 day, which has almost half wave length lags, but the amplitudes are very weak. Occurrence days of 5 m/s strong wind at Kototabang increase after maximum convective activity and have two peaks at +3 and +17 day. The peak of mean daily rainfalls correspond to T_{BB} minimum and increase around 1.5 times of average daily rainfalls. The occurrence of rainy days is always more than 50% and 10–20% increase during active phase of ISO.

Figure 4.18 represent time-longitude cross-sections for 20–90-day filtered GMS T_{BB} data and NCEP 700 hPa zonal wind. Days written in Table 4.2 are utilized as base days. The amplitude of T_{BB} is weakened at 100°E, which is consistent previous analysis results. Average phase speed of T_{BB} is around 6 m/s, but the phase speed tend to be slowly after passing through 120°E and enter western Pacific warm pool region. For zonal wind, between 70–120°E phase speeds are same as that of T_{BB} and phase is proceeding around 10 days. At the east of 120°E westerly wind anomalies extend rapidly eastward. Sui and Lau (1992) analyzed east Indian–western Pacific ocean region in 1979 of northern winter concerning intraseasonal oscillation and higher frequency disturbances. The slow propagation of cloud systems in western Pacific region is consistent to their results. They also showed that the strong westerly extend to wide regions between 140°E and date line.

4.4 Discussions

In this chapter relationship between westerly wind speed and precipitation, which appeared in case studies described in Chapter 3, is examined by utilizing longer dataset during August 1999–April 2002. The dominant wind direction at Kototabang is north-westerly and strong wind appear in westerly(Fig. 4.1). In this analysis zonal wind speeds are utilized to simplified the discussion. Strong zonal wind nearly correspond to westerly as strong easterly is scarce. Most of total rainfall amounts occupied by weak westerly periods, and moreover, the precipitation percentages are also large (Fig. 4.3). The rate of precipitation for strong westerly has minimum at 6 m/s and increase as wind speed become strong (Fig. 4.3). This indicates two possibilities.

i) There are two different cloud systems affected rainfalls to Kototabang. The cloud systems which dominate under weak wind conditions tend to suppress or rarely occur under strong wind, vice versa.

ii) It tends to occur convectively suppressed conditions under moderate zonal wind condition (4–8 m/s).

In Section 4.2 differences of cloud systems under weak and strong wind were investigated. At first each maximum daily rainfall days are analyzed. The rainfall of weak day occurred in the afternoon and intense rainfall occurred in a short time. The rainfall of strong day was long-lasting rainfall (Fig. 4.4). However, the mean diurnal variation of rainfalls at Kototabang are generally dominant in both conditions and afternoon rainfalls during 14–18 LST are dominant (Figs. 4.7 and 4.8). The diurnal variations of T_{BB} above Kototabang are also dominant and become minimum (or cloud top heights become highest) during 18–23 LST (Fig. 4.10) under both weak and strong westerly conditions. The remarkable differences between weak and strong westerly days are cloud top height in the daytime (6–18 LST). On one hand, weak westerly days ranges of 270–290 K are most frequent, which nearly correspond to the surface. On the other hand, T_{BB} of 250–270 K frequently appears in strong westerly days. This implies the ground tends to cover clouds in the daytime. The obvious diurnal variations of T_{BB} distributions appears in both conditions, which are most frequencies of less than 230 K in land regions at 12Z, coastal regions (till around 200 km from the land coasts) at 00Z, and oceanic regions (more than 200 km offshore regions) at 06 Z. In weak westerly days westward propagation of convections from Sumatera mountain range are clearly seen in the equatorial eastern Indian Ocean (propagating speed is around 8 m/s). These are similar to past studies (e.g., Nitta and Sekine, 1994). In strong westerly days, the places and time of active convections are almost same as weak westerly days, but convections in the oceanic regions are more active than that in weak westerly days. The cloud development on Sumatera mountain range during strong westerly periods and diurnal variation of rainfall at Kototabang implies that the diurnal variations are also important on strong westerly conditions, and the strong wind does not contribute suppression of local-scale cloud systems, which suggested in Section 3.1. The possibility that cloud activities are suppressed under strong wind, are obtained in case studies (see Chapter 3.3).

The relationships between westerly and precipitation on seasonal and intraseasonal time scale are discussed in Section 4.3. The periodicities of 10-day and 30–50 day are dominant

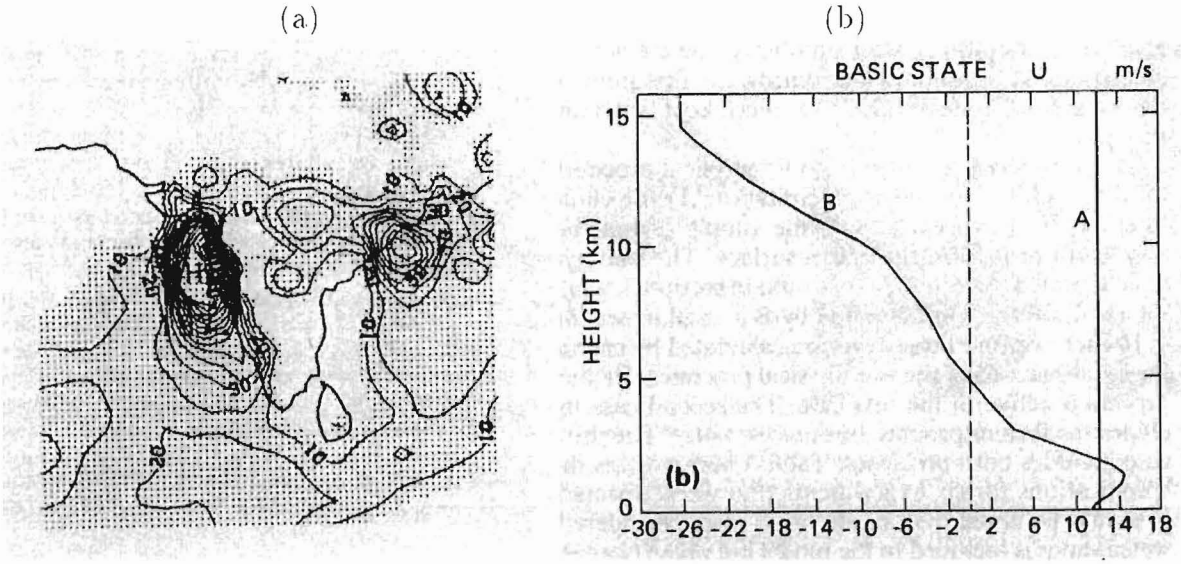

Figure 4.19: (a) the precipitation intensity (mm/day) estimated from satellite over India and the Arabian Sea on 24 June 1979 and (b) the vertical profile (after Ogura and Yoshizaki, 1988).

on the spectral analysis of rainfalls at Kototabang, NCEP 700 hPa zonal wind at nearest grid point at Kototabang and GMS T_{BB} above Kototabang (Fig. 4.15). The periodicity of 10-day coincident with the quasi-10-day disturbances appeared in September–October 1998 (Section 3.1). The periodicity of 30–50 days is considered as ISOs. The composite analysis based on the 20–90-day bandpass filtered minimum T_{BB} at (90°E, 0°) indicate around 50% increase of rainfalls for mean daily rainfall amount in active phase of ISO. The rate of rainy days also increase around 10% compared with the mean rate. On the other hand, the strong westerly days have two peaks around 5 and 15 days after active phase of ISO, which implies that the existence of other factors which bring strong westerly.

It is known that ISOs are sometimes depressed in the Indonesian maritime continent. Nitta *et al.*considered that the strong westerly which follows to ISO was blocked by Sumatera mountain range. In Section 3.1 as the explanation of the weak influence of ISO in the Indian Ocean on rainfalls at Kototabang, it was suggested that the location of Kototabang was the east of mountain range and most of rainfalls were occurred in the western side. However, it might be reasonable to regard the location of Kototabang as mountainous region because elevation of Kototabang is 865 m, although about 1000 m mountains exist between Ocean and Kototabang. The active convections often appear in the Indian Ocean adjacent to Sumatera Island (e.g., Figs. 3.8 and 3.14). The similar phenomena that the rainfalls on mountain range are not so much and developed clouds distribute on the adjacent Ocean have been studied at India during mature monsoon season. Figure 4.19 is (a) the precipitation intensity (mm/day) estimated from satellite over India and the Arabian Sea on 24 June 1979, and (b) the vertical profile of the east–west component of the wind (After Ogura and Yoshizaki 1988). The period is correspond to mature period of monsoon and strong southwesterly blows toward the west

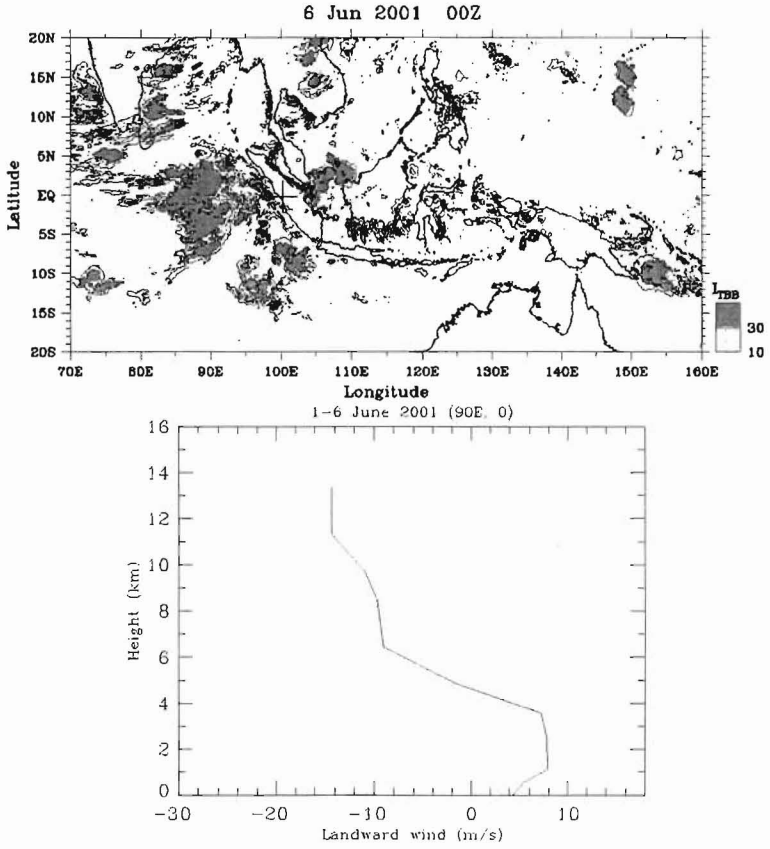

Figure 4.20: (a) The distribution of GMS T_{BB} data on 6 June 2001. (b) The averaged vertical wind profiles during 1–6 June 2001 at (0°90°E) drawn by NCEP reanalysis data

coast of India. However, maximum rainfalls occur over offshore region and not over the Western Ghat mountains. Grossman and Durran(1984) investigated interactions of low-level flow with the Western Ghats utilizing observational data, discussed by a nonlinear model and concluded that the Western Ghats produced offshore convections by gently lifting potential unstable air. Ogura and Yoshizaki (1988) argued by a two-dimensional compressible moist cloud model and concluded that in addition to lifting effect of mountain, strongly sheared flows and fluxes of latent and sensible heat from the ocean are essential to explain the observed features of rainfalls over the Arabian Sea and the Ghat Mountains.

It is compared the studies of rainfalls over the Arabian Sea and the Ghat Mountains during monsoon periods with the rainfalls at Kototabang, clouds distributions around Sumatera Island, and vertical structures of wind during active phase of ISOs over east Indian Ocean and Sumatera Island. There are some similarities between the Ghat Mountains and the mountain range of Sumatera. Firstly, both mountains distribute along the west coast of the land. Secondly, Sumatera Island experience strong westerlies in lower troposphere and upper level strong easterly when large cloud disturbances by ISOs become active over eastern equatorial Indian Ocean. These points satisfied the conditions of activating offshore convections suggested by Gross and Duran (1984) and Ogura and Yoshizaki (1988). Then it is possible that the lifting

effects of mountain range of Sumatera activate offshore convections in Indian Ocean.

The context of this chapter will be submitted as Murata *et al.*(2003).

Chapter 5

Summary and conclusions

This thesis has been described concerning the variations of rainfalls at Kototabang (100.32°E, 0.2°S, 865m MSL), West Sumatera, Indonesia and especially, on the relationship with the low tropospheric westerly wind.

In Chapter 1, the foregoing studies concerning the cloud activities in tropical regions within time scales of 30–60 days corresponding to intraseasonal oscillations(ISOs) and related studies for the tropospheric zonal wind variations have been reviewed. In addition, the past investigations on diurnal variations of convective cloud and precipitation, and on orographic precipitation have been described. Finally, the observational efforts to understand the weather and climate of Indonesia were introduced.

In Chapter 2, the observations and measurements employed in this thesis, have been described. It has been shown that the data of echo power and vertical Doppler velocity of the boundary layer radar(BLR) can provide a determination method of rainfall. The horizontal wind data of BLR are shown to be consistent with the NCEP reanalysis.

In Section 3.1, the observational results during September–October 1998 including an intensive observation period and plausible explanations have been mentioned. The most important issue in this thesis, a correlation between precipitation and lower tropospheric westerly, have been analyzed and described. The precipitation at Kototabang is mainly due to the local cloud systems developed on the mountainous regions (Barisan Mountains) and the cloud systems cannot be developed under strong westerly wind, because the local circulations are suppressed. Discussions on the causes of zonal wind variations observed in this period and the possible effect on the precipitation at Kototabang have been also described in Section 3.2.

In Section 3.3, it has been described that the results of another intensive observation period during May–June 2001 also showed similar results to the previous case study, as well as new findings such as a little lag between strong westerly and stoppage of precipitation.

In Chapter 4, the correlation between low-level westerly and precipitation at Kototabang has been examined by using nearly three-year data. The results statistically have indicated that the precipitation at Kototabang tends to occur when the westerly wind is less than 5 m/s. The analysis for days with precipitation larger than 30 mm has revealed that the precipitation by local cloud systems generated with a diurnal cycle prevails at Kototabang. Not much cases of the large-scale cloud disturbances associated with ISOs lead a possibility of the lifting effect of Barisan Mountains on the convections off the west coast of Sumatera, from the similarity to the studies of Western Ghats Mountains in India.

The main conclusions of this thesis are as follows:

- The precipitation at Kototabang occurs with a high probability when the westerly wind is less than 5 m/s.
- The precipitation by local cloud systems developed in the afternoon prevails at Kototabang.
- The observational results at Kototabang lead a possibility of the lifting effect of Barisan Mountains on the convections off the west coast of Sumatera.

These results obviously indicate differences from the foregoing many investigations for the variations of oceanic convections and reveal the importance of orographic effects on the tropical convective activities.

To improve the reliability of the results described in this study it is necessary to compare with observational results of other stations around Sumatera mountain range and offshore regions, because this study mainly based on observational results of a single station. Especially, understanding of the structures of local circulations and their connections to the local cloud systems in Sumatera Island is required. We believe that these observational studies must contribute to understand behavior of convective activities in Indonesian region more precisely and enable to forecast tropical weather in the future.

References

Chen, S. S., and R. A. Houze Jr., 1997: Diurnal variation and life-cycle of deep convective systems over the tropical Pacific warm pool. *Quart. J. Roy. Meteor. Soc.*, **123**, 357–388.

Fujibe, F., 1999: Diurnal variation in the frequency of heavy precipitation in Japan. *J. Meteor. Soc. Japan*, **77**, 1137–1149.

Fujiwara, M., K. Kita and T. Ogawa, 1998: Stratosphere-troposphere exchange of ozone associated with the equatorial Kelvin wave as observed with ozonesondes and rawinsondes. *J. Geophys. Res.*, **103**, 19173–19182.

Fujiwara, M., K. Kita, T. Ogawa, S. Kawakami, T. Sano, N. Komala, S. Saraspriya and A, Suripto, 2000: Seasonal variation of troposphere ozone in Indonesia revealed by 5-year ground-based observations. *J. Geophys. Res.*, **105**,1879–1888.

Gage, K. S, 1990: Radar observations of the free atmosphere: Structure and dynamics. *Radar in Meteorology: Battan Memorial and 40th Anniversary Radar Meteorology Conference*, edited by D. Atlas, American Meteorological Society, 534–565.

Gray, W. M. and R. W. Jacobson, Jr., 1977: Diurnal variation of deep cumulus convection. *Mon. Wea. Rev.*, **105**, 1171–1188.

Hamada, J. -I., M. D. Yamanaka, J. Matsumoto, S. Fukao, P. A. Winarso and T. Sribimawati, 2002: Spatial and temporal variations of the rainy season over Indonesia and their link to ENSO. *J. Meteor. Soc. Japan*, **80**, 285–310.

Hashiguchi, H., S. Fukao, T. Tsuda, M. D. Yamanaka, D. L. Tobing, T. Sribimawati, S. W. B. Harijono and H, Wiryosumarto, 1995: Observations of the planetary boundary layer over equatorial Indonesia with an *L*-band clear-air doppler radar: Initial results. *Radio Sci.*, **30**, 1,043–1,054.

Hashiguchi, H., S. Fukao, M. D. Yamanaka, S. W. B. Harijono and H, Wiryosumarto, 1996: An overview of the planetary boundary layer observations over equatorial Indonesia with an *L*-band clear-air doppler radar. *Beitr. Phys. Atomosph.*, **69**, 13–25.

Hendon, H. H. and K. Woodberry, 1993: The diurnal cycle of tropical convection. *J. Geophys. Res.*, **98**, 16623–16637.

Holton, J. R., 1992: An introduction to dynamic meteorology. 3rd ed. Academic Press, 511pp.

Houze Jr., R. A., S. G. Geotis, F. D. Marks Jr. and A. K. West, 1981: Winter Monsoon convection in the vicinity of north Borneo. Part I: Structure and time variation of the cloud and precipitation. *Mon. Wea. Rev.*, **109**, 1595–1614.

Inoue T. and K. Nakamura, 1990: Physical and Biological Background for Insect Studies in Sumatra. *Natural History of Social Wasps and Bees in Equatorial Sumatra*, edited by Sh. F. Sakagami, R. Ohgushi and D.W.Roubik, Hokkaido University Press, Sapporo, Japan, 274pp.

Keen, R. A., 1982: The role of cross-equatorial tropical cyclone pairs in the Southern Oscillation. *Mon. Wea. Rev.*, **110**, 1405–1416.

Keen, R. A., 1988: Equatorial westerlies and the Southern Oscillation.. Proc. U.S. TOGA Western Pacific Air-Sea Interaction Workshop, Honolulu, R.Lukas and P. Webster, Eds., U.S.TOGA Rept. USTOGA-8, University Corporation of Atmospheric Reserch,.

Kubota, H. and T. Nitta, 2001: Diurnal variations of tropical convection observed during the TOGA-COARE. *J. Meteor. Soc. Japan*, 815–830.

Lau, K. M., L. Peng, C. H. Sui and T. Nakazawa, 1989: Dynamics of super cloud clusters,westerly wind bursts, 30-60 day oscillations and ENSO: an unified view. *J. Meteor. Soc. Japan*, **67**, 205–219

Lin, X. and R. H. Johnson, 1996: Kinematic and thermodynamic characteristics of the flow over the western Pacific warm pool during TOGA COARE. *J. Atmos. Sci.*, **53**, 695–715.

Madden, R. A. and P. R. Julian, 1971: Detection of a 40–50 day oscillation in the zonal wind in the tropical pacific. *J. Atmos. Sci.*, **28**, 702–708

Madden, R. A. and P. R. Julian, 1972: Description of global-scale circulation cells in the tropics with a 40–50 day period. *J. Atmos. Sci.*, **29**, 1109–1123.

Matsumoto, J., 1992: The seasonal changes in Asian and Australian monsoon region. *J. Meteor. Soc. Japan*, **70**, 257–272.

Matsuno, T., 1966: Quasi-geostrophic motions in the equatorial area. *J. Meteor. Soc. Japan*, **44**, 25–43.

Murakami, T. and J. Matsumoto, 1994: Summer monsoon over the Asian continent and western north Pacific. *J. Meteor. Soc. Japan*, **72**, 719–745.

Murata, F., M. D. Yamanaka, M. Fujiwara, S. -Y. Ogino, H. Hashiguchi, S. Fukao, M. Kudsy, T. Sribimawati, S. W. B. Harijono and E. Kelana, 2002: Relationship between wind and precipitation observed with a UHF radar, GPS rawinsondes and surface meteorological instruments at Kototabang, West Sumatera during September–October 1998. *J. Meteor. Soc. Japan*, **80**, 347–360.

Murata, F., M. D. Yamanaka, S. -Y. Ogino, M. Fujiwara, H. Hashiguchi, S. Fukao, M. Kudsy, T. Sribimawati, S. W. B. Harijono and B. Suhardi, 2003: Two types of rainfall at Kototabang, West Sumatera, Indonesia: A statistical study based on observations for 33 months. *J. Meteor. Soc. Japan, submitted.*

Nakazawa, T., 1988: Tropical super cloud clusters within intraseasonal variations over the western pacific. *J. Meteor. Soc. Japan*, **66**, 823–839.

Nishi, N. and A. Sumi, 1995: Eastward-moving disturbance near the tropopause along the equator during the TOGA COARE IOP. *J. Meteor. Soc. Japan*, **73**, 321–337.

Nitta, Ts. and T. Motoki, 1987: Abrupt enhancement of convective activity and low-level westerly wind burst during the onset phase of 1986-87 El Niño. *J. Meteor. Soc. Japan*, **65**, 497–506.

Nitta, Ts. and S. Sekine, 1994: Diurnal variation of convective activity over the tropical western pacific. *J. Meteor. Soc. Japan*, **72**, 627–641.

Nitta, Ts., T. Mizuno and K. Takahashi, 1992: Multi-scale convective systems during the initial phase of the 1986/87 El Niño. *J. Meteor. Soc. Japan*, **70**, 448–466.

Numaguti, A., R. Oki, K. Nakamura, K. Tsuboki, N, Misawa, T. Asai and Y. -M. Kodama, 1995: 4-5-day-period variation and low-level dry air observed in the equatorial western Pacific during the TOGA-COARE IOP.. *J. Meteor. Soc. Japan*, **73**, 267–290.

Ohsawa, T., H. Ueda, T. Hayashi, A. Watanabe and J. Matsumoto, 2001: Diurnal variations of convective activity and rainfall in tropical Asia. *J. Meteor. Soc. Japan*, **79**, 333–352.

Okamoto, N., M. D. Yamanaka, S. -Y. Ogino, H. Hashiguchi, N. Nishi, T. Sribimawati and A. Numaguchi, 2002: Seasonal variations of tropospheric wind over Indonesia: Comparison between collected operational rawinsonde data and NCEP reanalysis for 1992–97. *J. Meteor. Soc. Japan, submitted.*

Oki, T. and K. Musiake, 1994: Seasonal change of the diurnal cycle of precipitation over Japan and Malaysia. *J. Appl. Meteor.*, **33**, 1445–1463.

Renggono, F., H. Hashiguchi, S. Fukao, M. D. Yamanaka, S. Ogino, N. Okamoto, F. Murata, B. P. Sitorus, M. Kudsy, M. Kartasasmita and G. Ibrahim, 2001: Precipitating clouds observed by L-band boundary layer radars in equatorial Indonesia. *Annales Geophysicae*, **19**, 889–897.

Shimizu, A. and T. Tsuda, 1997: Characteristics of Kelvin waves and gravity waves observed with radiosondes over Indonesia. *J. Geophys. Res.*, **102**, 26159–26171.

Sui, C. -H. and K. M. Lau, 1992: Multiscale phenomena in the tropical atmosphere over the western Pacific. *Mon. Wea. Rev.*, **120**, 407–430.

Takayabu, Y. N. and K. M. Lau and C. H. Sui, 1996: Observation of a quasi-2-day wave during TOGA COARE. *Mon. Wea. Rev.*, **124**,1892–1913.

Takayabu, Y. N., 1994: Large-scale cloud disturbances associated with equatorial waves. part 1: spectral features of the cloud disturbances. *J. Meteor. Soc. Japan*, **72**,433–449.

Tsuda, T., Murayama, H. Wiryosumarto, S. W. B. Harijono, and S. Kato, 1994: Radiosonde observations of equatorial atmosphere dynamics over Indonesia, 1, Equatorial waves and diurnal tides. *J. Geophys. Res.*, **99**,10491–10505.

Wallace, J. M. and V. E. Kousky, 1968: Observational evidence of Kelvin waves in the tropical stratosphere. *J. Atmos. Sci.*, **25**, 900–907.

Webster, P. J. and R. Lukas, 1992: TOGA COARE: The Coupled Ocean–Atmosphere Responde Experiment. *Bull. Amer. Meteor. Soc.*, **73**, 1377–1416.

Wheeler M. and G. N. Kiladis, 1999: Convectively coupled equatorial waves: analysis of cloud and temperature in the wavenumber–frequency domain. *J. Atmos. Sci.*, **56**, 374–399.

Wheeler M., G. N. Kiladis, P. J. Webster, 2000: Large-scale dyamical fields associated with convectively coupled equatorial waves. *J. Atmos. Sci.*, **57**, 613–640.

Widiyatmi, I., M. D. Yamanaka. H, Hashiguchi, S. Fukao, T, Tsuda, S.-Y. Ogino, S. W. B. Harijono and H. Wiryosumato, 1999: Quasi 4 day mode observed by a boundary layer radar at Serpong (6°S, 107°E), Indonesia. *J. Meteor. Soc. Japan*, **77**, 1117–1184.

Yanai, M. and T. Maruyama, 1966: Stratospheric wave disturbances propagating over the equatorial Pacific. *J. Meteor. Soc. Japan*, **44**, 291–294.

Yanai, M., B. Chen and W. -W. Tung, 2000: The Madden–Julian oscillation observed during the TOGA COARE IOP: Global view. *J. Atmos. Sci.*, **57**, 2374–2396.

Publication list

Refereed journals

i) Renggono, F., H. Hashiguchi, S. Fukao, M. D. Yamanaka, S. -Y. Ogino, N. Okamoto, F. Murata, B. P. Sitorus, M. Kudsy, M. Kartasasmita, and G. Ibrahim, Precipitating clouds observed by 1.3 GHz boundary layer radars in equatorial Indonesia, *Annales Geophysicae*, **19**, 889–897, 2001.

ii) Murata, F., M. D. Yamanaka, M. Fujiwara, S. -Y. Ogino, H. Hashiguchi, S. Fukao, M. Kudsy, T. Sribimawati, S. W. B. Harijonom and E. Kelana, Relationship between wind and precipitation observed with UHF radar, GPS rawinsondes and surface meteorological instrument at Kototabang, West Sumatera Indonesia during September–October 1998, *J. Meteor. Soc. Japan*, **80**, 347–360, 2002.

iii) Mori, S., J. -I. Hamada, Y. I. Tauhid, N. Okamoto, F. Murata, R. Araki, N. Sakurai, T. Okuda, T. Sribimawati, U. Haryoko, B. Suhardi, Emrizal, P. M. Wu, K. Ichiyanagi, H. Hashiguchi, M. D. Yamanaka, and T. Yasunari, The crossroads of atmospheric circulations over the Indonesian maritime continent: intense observations in Sumatera, *J. Meteor. Soc. Japan*, submitted, 2003.

iv) Murata, F., M. D. Yamanaka, S. Mori, J. -I. Hamada, Y. I. Tauhid, H. Hashiguchi, M. Kudsy, T. Sribimawati, S. W. B. Harijono, and B. Wiryosumarto, Relationship between low-level westerly wind and dry air observed at Kototabang, West Sumatera during May–June, 2001, *J. Meteor. Soc. Japan*, submitted, 2003.

v) Murata, F., M. D. Yamanaka, S. -Y. Ogino, M. Fujiwara, H. Hashiguchi, T. Sribimawati, and B. Suhardi, Main precipitating systems and its relation to low tropospheric westerlies at Kototabang, West Sumatera, *J. Meteor. Soc. Japan*, submitted, 2003.

Unrefereed articles

i) Murata, F., M. D. Yamanaka, F. Fujiwara, S. -Y. Ogino, H. Hashiguchi, J. -I. Hamada, S. Fukao, T. Sribimawati, M. Kudsy, S. W. B. Harijono, and E. Kelana, Temporal variations of convective clouds and precipitations in Indonesia, *Preprints of the Third GEWEX International conference, Beijing, June*, 1999. 95

ii) Murata, F., M. D. Yamanaka, M. Fujiwara, S. -Y. Ogino, H. Hashiguchi, J. -I. Hamada, S. Fukao, T. Sribimawati, M. Kudsy, S. B. W. Harijono, and E. Kelana, Observations of precipitating cloud systems with UHF radar, GPS rawinsondes and surface meteorological instruments at Bukit Kototabang, West Sumatera during September–October 1998,

BIBLE workship aircraft and ground measurement in Indonesia and Australia, Tokyo, July, 1999.

iii) Murata, F., M. D. Yamanaka, M. Fujiwara, S. -Y. Ogino, H. Hashiguchi, J. -I. Hamada, S. Fukao, T. Sribimawati, M. Kudsy, S. B. W. Harijono, and E. Kelana, Observations of precipitating clouds at Bkt. Kototabang, *Proceedings of the 2nd International conference on science and technology for the assessment of global climate change and its impacts on Indonesian maritime continent., Jakarta, December*, 1999. A4.1

iv) Murata, F., M. D. Yamanaka, H. Hashiguchi, S. -Y. Ogino, S. Fukao, M. Fujiwara, T. Ohsawa, E. Kelana, T. Sribimawati, M. Kudsy, and S. W. B. Harijono, Observations of precipitating clouds at Bukittinggi, West Sumatera, Indonesia, Ninth international workshop on technical and scientific aspects of MST radar., Toulouse, 361–364, 2000.

v) Murata, F., S. -Y. Ogino, M. D. Yamanaka, M. Fujiwara, H. Hashiguchi, S. Fukao, T. Sribimawati, M. Kudsy, S. W. B. Harijono, and E. Kelana, Relationship between wind and precipitation observed with a UHF radar, GPS rawinsondes and surface meteorological instrument at Kototabang, West Sumatera during September–October 1998, *Proceedings of IAMAS, Innsbruck, July*, 2001. 63

vi) Murata, F., S. -Y. Ogino, M. D. Yamanaka, M. Fujiwara, H. Hashiguchi, S. Fukao, T. Sribimawati, M. Kudsy, S. W. B. Harijono, and E. Kelana, Relationship between wind and precipitation observed with a UHF radar, GPS rawinsondes and surface meteorological instrument at Kototabang, West Sumatera during September–October 1998, *Proceedings of 5th International GAME Conference, Nagoya, October*, 2001. 77–80

vii) Murata, F., S. -Y. Ogino, M. D. Yamanaka, M. Fujiwara, H. Hashiguchi, S. Fukao, T. Sribimawati, M. Kudsy, S. W. B. Harijono, and E. Kelana, Relationship between wind and precipitation observed with a UHF radar, GPS rawinsondes and surface meteorological instrument at Kototabang, West Sumatera during September–October 1998, *Proceedings of EPIC symposium, Kyoto, March*, 10, 2002.

viii) Murata, F., M. D. Yamanaka, S. -Y. Ogino, M. Fujiwara, H. Hashiguchi, S. Fukao, S. Mori, J. -I. Hamada, Y. I. Tauhid, T. Sribimawati, and E. Kelana, Observational results for relationship between lower tropospheric westerly and rainfall at Kototabang, West Sumatera, Indonesia, *Proceedings of IUGG. Sapporo, July*, 2003.